Available online at www.sciencedirect.com
ScienceDirect
Physics of the Earth and Planetary Interiors 161 (2007) 50–73
PHYSICS OF THE EARTH AND PLANETARY INTERIORS
www.elsevier.com/locate/pepi

Palaeomagnetic and rock magnetic properties of travertine: Its potential as a recorder of geomagnetic palaeosecular variation, environmental change and earthquake activity in the Sıcak Çermik geothermal field, Turkey

John D.A. Piper [a,*], Levent B. Mesci [b], Halil Gürsoy [b], Orhan Tatar [b], Ceri J. Davies [a]

[a] *Geomagnetism Laboratory, Department of Earth and Ocean Sciences, University of Liverpool, Liverpool L69 7ZE, UK*
[b] *Department of Geology, Cumhuriyet University, 58140 Sivas, Turkey*

Received 10 January 2006; received in revised form 5 January 2007; accepted 6 January 2007

Abstract

Travertine, the product of incremental growth of inorganic carbonate, is potentially a high-resolution recorder of geomagnetic palaeosecular variation (PSV) when it incorporates small amounts of ferromagnetic material. It grows most regularly in regions of neotectonic activity where geothermal waters feed into extensional fissures and deposit successive layers of carbonate as *fissure travertine*. The same waters spill out onto the surface to deposit *bedded travertine* which may incorporate wind blown dust including ferromagnetic particles. Tectonic travertine deposits are linked to earthquake activity because the geothermal reservoirs are reset and activated by earthquake fracturing but tend to become sealed up by carbonate deposition between events. This study investigates whether sequential deposition can identify cycles of PSV and provide a means of estimating rates of travertine growth and earthquake frequency. The palaeomagnetic record in three travertine fissures from the Sıcak Çermik geothermal field in Central Anatolia and nearby bedded travertines dated up to 360,000 years in age (U–Th) are investigated to evaluate magnetic properties and relate the geomagnetic signature to earthquake-induced layering.

Sequential sampling of bedded travertine from the margins (earliest deposition) to centres of fissures (last deposition) identifies directional migrations reminiscent of PSV. Thermal demagnetisation shows that goethite pigment is not a significant remanence carrier; instead hematite, and more rarely magnetite, is the carrier. Magnetic susceptibility of fissure travertine is proportional to the calcite:aragonite ratio. Two-frequency susceptibility analysis identifies a ferromagnetic content in bedded travertine dominated by fine superparamagnetic grain sizes whereas the fissure travertine has mostly single and multidomain grain sizes, a difference interpreted to reflect contrasting energies of the two environments plus atmospheric input in the bedded travertine. Fissure travertine possesses strong lineated anisotropy of magnetic susceptibility (AMS), with horizontal k_{max} axes oriented along the fissure axes and k_{int} and k_{min} distributed within the orthogonal plane; this is explained by rolling of ferromagnetic grains up the side of the fissure during repeated water ejection until fixed by the host carbonate precipitation. In contrast bedded travertine has low magnitude AMS with near neutral ellipsoid shapes controlled by settling of grains during weak outflow from the axis of the fissure ridge. The source of the magnetic minerals in the fissure travertine is probably in material washed down by meteoric waters from the local terra rossa soil and concentrations of these minerals (and hence magnetic susceptibility) could be a signature of pluvial environments. Fissure travertine is a reliable recorder of the ambient field when layered although bedded travertine is found to exhibit inclination shallowing. On the assumption that PSV cycles record periods of 1–2 ky, layering in the travertine identifies resetting of the geothermal system by earthquakes every 50–100 years in this region. Travertine precipitation occurs at rates of 0.1–0.3 mm/year on each side of the

* Corresponding author. Tel.: +44 151 794 2000; fax: +44 151 708 6502.
E-mail address: sg04@liverpool.ac.uk (J.D.A. Piper).

0031-9201/$ – see front matter
doi:10.1016/j.pepi.2007.01.006

extensional fissures and possibly at a rate an order higher as bedded travertine on the surface. Earthquakes of magnitude $M \leq 4$ occur much too frequently to have any apparent influence on travertine deposition but earthquakes with $M = 4.5$–5.5 occur with a frequency compatible with the travertine layering and appear to be the events recorded by the layering. Two signatures of much larger earthquakes on a 1–10 ky timescale are also recorded by travertine deposition. These are (i) incidental emplacement of massive travertine or fracturing of earlier travertine without destruction of the fissure as a venue of travertine emplacement and (ii) termination of the fissure as a site of deposition with transfer of geothermal activity to a new fracture. Palaeomagnetic estimates of fissure duration and the presence of some 25 fractures in the ~300,000 year old Sıcak Çermik field growing at rates of 0.1–0.6 mm/year suggests that the type (ii) signature is achieved by an $M \sim 7.5$ event approximately every 10,000 years.

Keywords: Travertine; Turkey; Palaeomagnetism; Palaeosecular variation; Earthquake frequency; Palaeoseismology; Magnetic fabric; Magnetic susceptibility; Neotectonics

1. Introduction

Geological recorders of palaeosecular variation (PSV) of the geomagnetic field need to fix the direction of the field during rapid and regular accumulation. Much use has been made of sediments deposited in lakes where seasonal input and rapid deposition may potentially provide a good recording medium (Thompson and Oldfield, 1986). Such materials are efficient recorders provided that diagenesis and bioturbation have not degraded the record and suggest that PSV is closely constrained to the Earth's rotation axis with complete cycles taking periods of the order of 1000–2000 years to complete (e.g. Tarling, 1988; Butler, 1992). Potential hard rock recorders include speleothems (Latham and Ford, 1993), although slow incrementation and climatically dependent growth limit their usefulness.

Currently little use has been made of travertine, the inorganic carbonate deposition from hydrothermal waters draining hinterland including limestone and dolomites, and deposited whenever the partial pressure of CO_2 is reduced. Travertine deposition occurs most actively and regularly in regions of neotectonism where the groundwater is frequently at elevated temperatures, thus enhancing solution of country rock, and extensional fissures are progressively filled in by *fissure travertine* as they are opened up by extension (Hancock et al., 1999). The incremental growths on each side of the fissure axis are then especially useful because they can be correlated with one another to evaluate temporal trends. Tectonically controlled travertine is usually layered (i.e. shows a sequential banding) because the hydrothermal system is episodically reset, and the flow stimulated, by earthquake activity; between earthquake events the geothermal reservoir is progressively sealed up by carbonate deposition and the flow reduced. Above the fissures the waters spill out onto the surface to deposit *bedded travertine* and build up a mound-like body (Fig. 1). The travertine here is a massive coherent deposit when the flow is vigorous but changes to a friable open textured deposit (*tufa*) as outflow wanes between earthquake events. Hence in regions of neotectonism travertine preserves a layered signature reflecting the past earthquake activity.

In this paper we report palaeomagnetic study of fissure fill travertine from a geothermal field in central Turkey with four objectives: (i) the major aim has been to investigate whether migrations of palaeofield direction occur that correlate with cycles of PSV. A comparison of these cycles with documented PSV behaviour may then allow rates of travertine growth can be estimated. (ii) Since the travertine deposits record a history of layering motivated by earthquake events, the numbers of layers within the PSV cycles may then be used to estimate the long-term earthquake frequency. We also note two longer term signatures in the travertine deposition which appear to define the incidence of much larger but infrequent earthquake events. (iii) Travertine may also potentially record an environmental signature because the magnetic grains are circulated into the groundwater from material flushed down through the soil (fissure travertine) with the addition of atmospheric deposition (bedded travertine). The signature of these ferromagnets is then a possible proxy for environmental change. (iv) Travertine is young material readily datable by the U–Th technique and the direction of magnetisation can then be used to monitor the rate and scale of neotectonic deformation.

2. Geological framework

The travertine used for this study is derived from the geothermal region of Sıcak Çermik (39.9°N, 36.9°E) 25 km west of the city of Sivas in central Turkey where hot springs permeate Upper Miocene-Lower Pliocene sediments (Ayaz and Gökçe, 1998). The carbonate source is probably marbles in underlying metamorphic

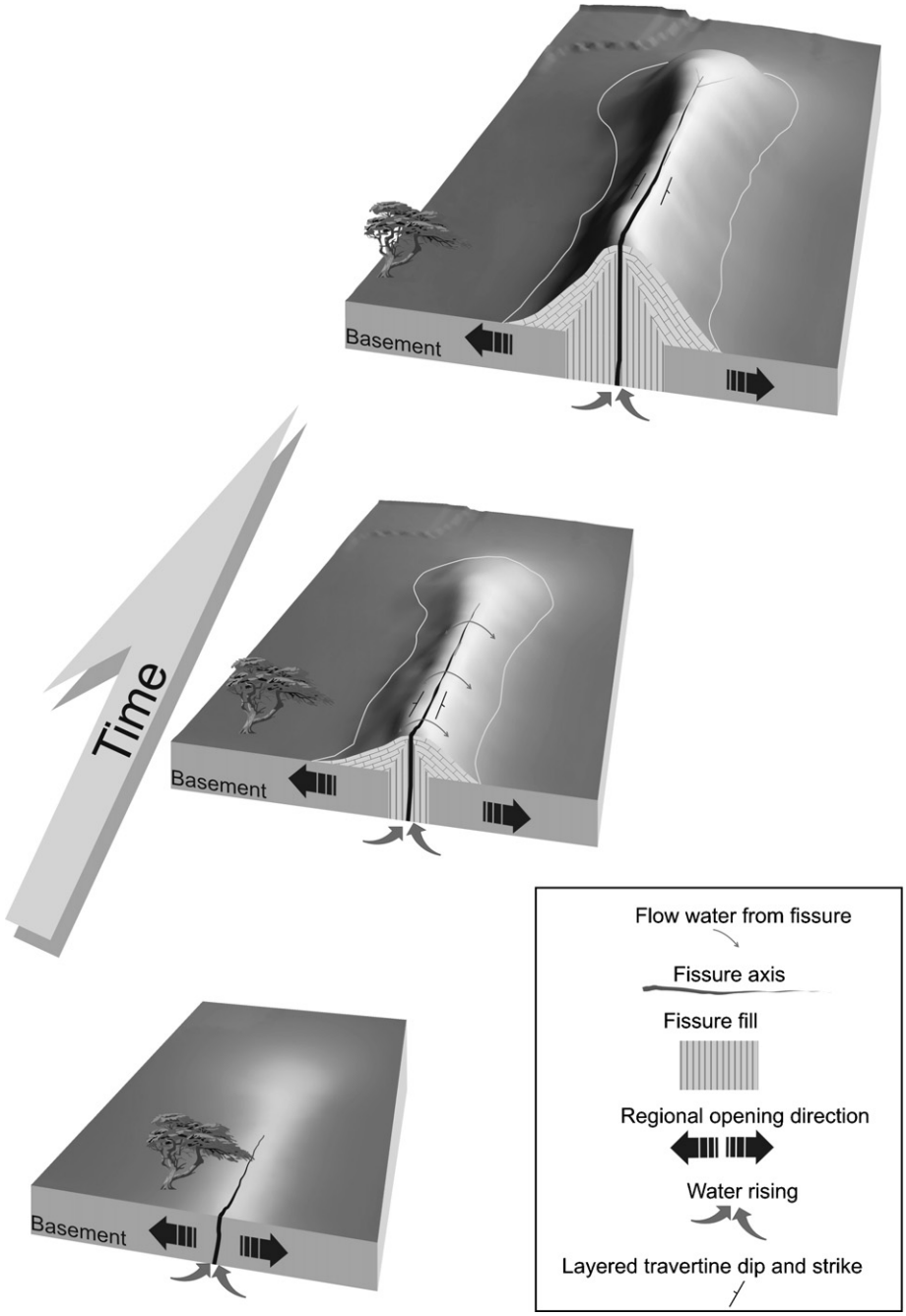

Fig. 1. Successive stages in the formation of a travertine mound above an extensional fissure (after Mesci, 2004).

rocks lying >100 m below the sediments. The regional tectonic regime is dominated by NNW-SSE compression (σ_1) resulting from the ongoing northward movement of Afro-Arabia into the Anatolides, an assemblage of accreted terranes between the Pontide Orogen at the Eurasian margin in the north and the Tauride Orogen in the south, although regional variations are complex due to the westward extrusion of fault blocks within Anatolia (Tatar et al., 1996; Gürsoy et al., 1997; Piper et al., 2006). The axis of minimum principal stress (σ_3) is a tension in this region and the sinuous pattern of fissure development (Fig. 2) appears to result from a torsional stress regime between two major NE–SW trending tear faults so that only the currently active fissures are

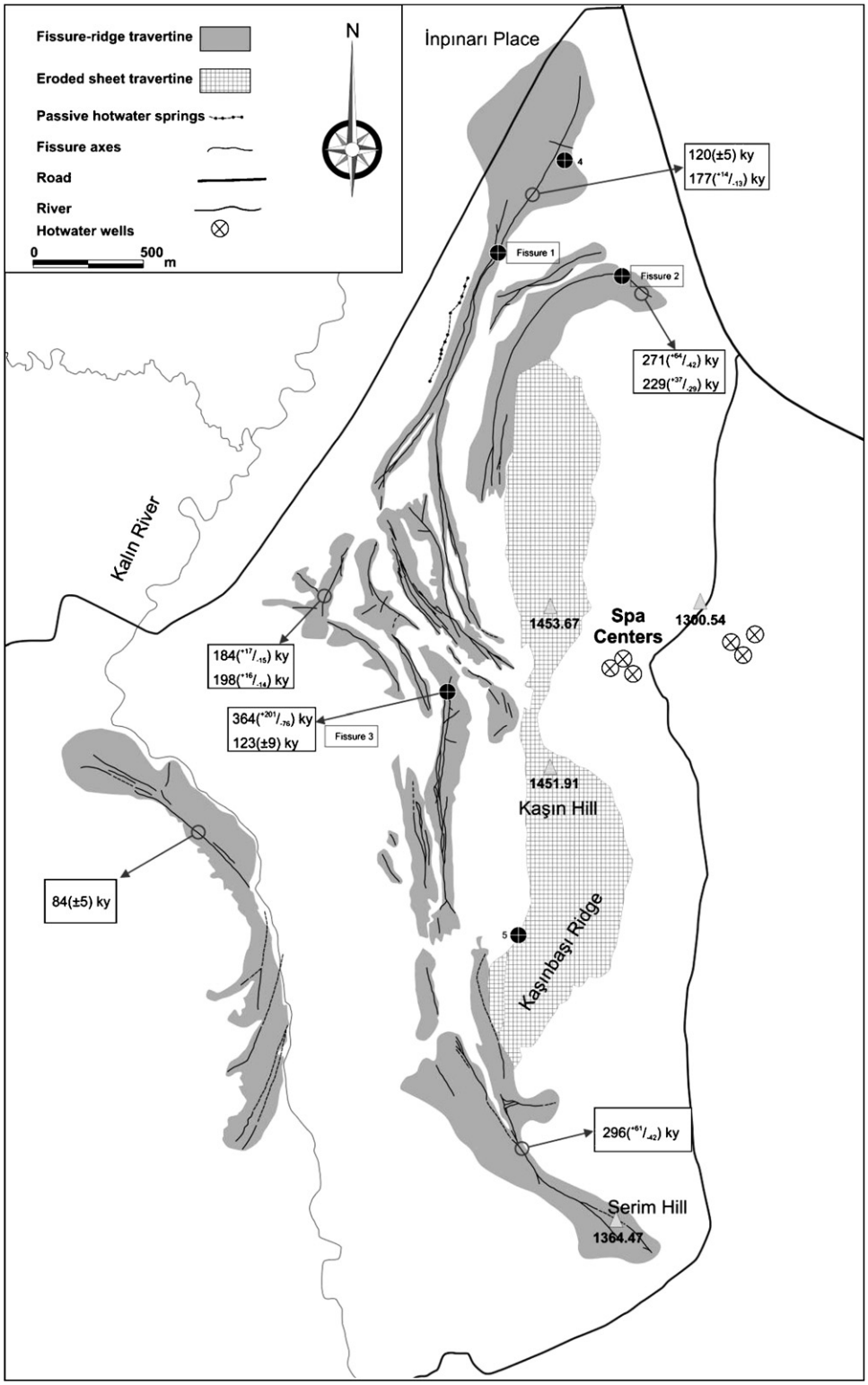

Fig. 2. Map of travertine distribution and tectonics in the Sıcak Çermik geothermal field near the city of Sivas, central Turkey after Mesci (2004). The locations of the three fissure travertines sampled for this study are shown with two additional sampled locations in bedded travertine (4 and 5).

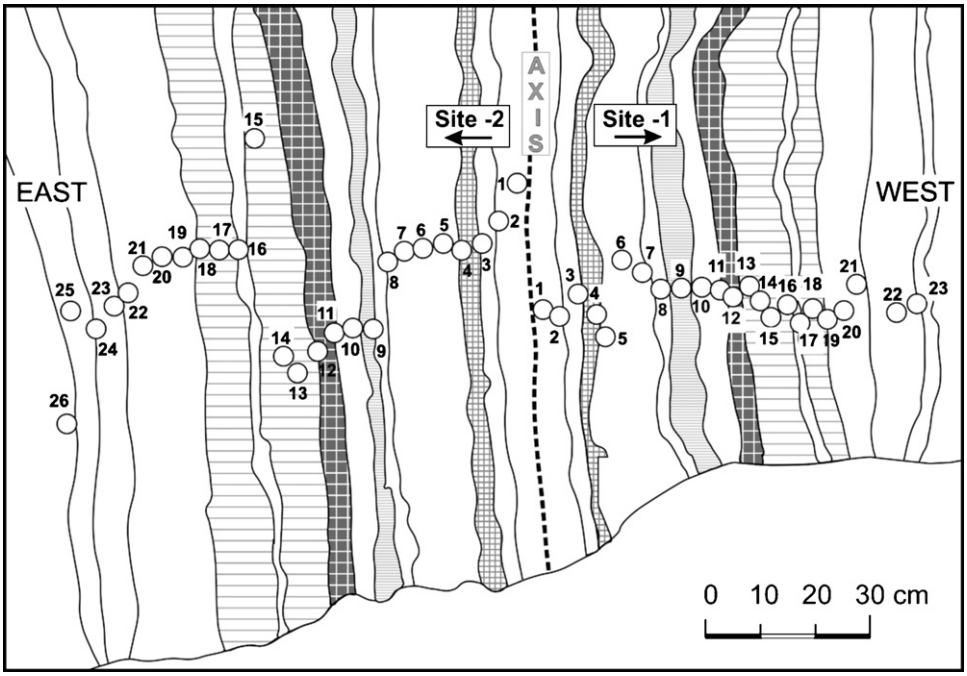

Fig. 3. Drawing from a photograph of Fissure 1 at Sıcak Çermik showing the system for sampling the palaeomagnetic cores outwards from the axis of the fissure. Note that key coloured bands can be matched on either side of the axis.

oriented NNW–SSE perpendicular to σ_3 (Mesci et al., 2007). Quarrying of mounds of layered travertine has excavated the sampled fissures and U–Th dating indicates that geothermal activity has occurred here, at least episodically, over the past 300–400 ky. The fissure fills consist of a succession of pale straight, sinuous or undulating carbonate bands interrupted by darker bands of varying shades of brown; the more prominent examples of the latter can be reliably matched on either side of the fissure axes. The fissures are either completely sealed or defined by a small gap showing that infilling by travertine occurred at approximately the same rate as the fissures were opened up by the regional extension.

3. Field and laboratory methods

Three travertine fissures were collected at localities denoted 1, 2 and 3 in Fig. 2 and drilled by coring outwards from the axes so that full thicknesses of travertine growth were sampled by successions of 2.4 cm diameter cores. At localities 1 and 2 suitable exposures enabled mirror sections to be sampled outwards on either side of the fissure axes (e.g. Fig. 3). Orientations were by both Sun and magnetic compasses. Much of the bedded travertine in this region comprises friable tufa and coherent samples proved difficult to core; isolated samples were obtained near the sampled fissures in addition to separate two locations (4 and 5) in more massive bedded travertine. Also for comparative work we have sampled 24 successive compact travertine layers from a travertine mound in a smaller geothermal field at Ortaköy near the town of Şarkışla 25 km SW of the Sıcak Çermik geothermal field.

The magnetisations in cores cut from field samples were determined by nitrogen SQUID (FIT) magnetometer following measurement of magnetic susceptibility using a Bartington Bridge. Progressive demagnetisation was applied to resolve components of magnetisation using either alternating field (a.f.) demagnetisation in steps of 5 or 10 milliTesla (mT) to peak fields of 140 mT or by thermal demagnetisation in steps of 25 or 50 °C. The preferred method of data analysis used orthogonal projections of the remanence vector onto horizontal and vertical planes accompanied by recognition of components by eye and calculation of equivalent directions of magnetisation by principal component analysis. The thermal demagnetisation could only be applied to ~350 °C due to disintegration of the carbonate host at higher temperatures, and directions of magnetisation were determined by end point analysis in samples showing stable behaviours where both methods of treatment produced minimal demagnetisation trajectories.

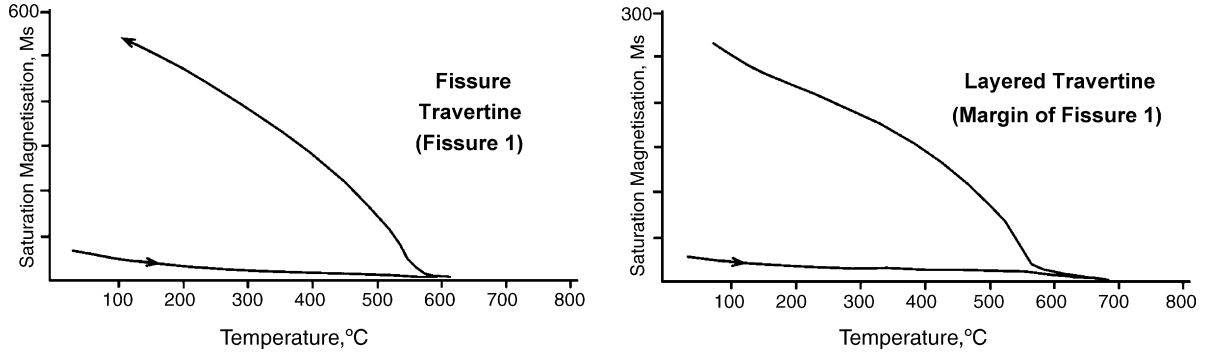

Fig. 4. Typical thermomagnetic determinations (saturation magnetisation M_s, vs. temperature) from a sample of fissure travertine (Fissure 1) and from an adjoining tufa sample of bedded travertine.

4. Rock magnetic properties

Saturation magnetisations (M_s) in travertine are very weak and thermomagnetic spectra mostly show convex and asymptotic curves obeying the Curie Law indicating that M_s is dominated by paramagnetism in the limonite pigment, and possible in siderite. A hematite Curie point is often discernible on the heating curves and magnetite inflections at ~580 °C were observed in some samples of the bedded travertine but were not detected in the fissure travertine. Low-Ti magnetite is produced by alteration during the cooling cycle, presumably from reduction of limonite or breakdown of siderite, and is reflected in large increase in M_s (Fig. 4).

Isothermal remanent magnetisations (IRMs) continue to be acquired to the limits of the laboratory field (2.7 Tesla) and show that much of the ferromagnetism in the travertine has high coercivities attributable to goethite, hematite or both. IRM acquisition can discriminate between multiple coercive force components if the magnetisation gradient is plotted against the log of the applied field (Robertson and France, 1994). The curve shape then isolates typical mean coercivities and the relative importance of each ferromagnetic component. This approach highlights the high coercivity minerals which dominate the ferromagnetism in fissure travertine, often with coercivities in excess of 2 Tesla, and sometimes comprising at least two phases (Fig. 5). There is indication of low coercivity material, presumably detrital magnetite, in the bedded travertine and tufa at Sıcak Çermik although only a high coercivity ferromagnetic was detected in the bedded travertine at Ortaköy (Fig. 5).

Magnetic susceptibility is significantly positive in all cores (which are therefore dominated by paramagnetism and/or ferromagnetism and not by the diamagnetic carbonate). This property shows some systematic variations across the fissures reflecting fluctuations in ferromagnetic input. In Fissure 1 there is a general decline in input towards the axis superimposed on large short term variations (Fig. 6). There is no marked correlation with limonitic staining (cf. Fig. 3) indicating that goethite is not the primary cause of the ferromagnetism. Fissure 2 shows weaker but more consistent susceptibilities between samples 7 and 37 on each side (Fig. 7) with indications of weaker ferromagnetic input at the beginning of travertine growth (around sample numbered 40) and at the waning stages of infill shortly before the fissure became extinct (cores 1–6).

Magnetic susceptibility was compared at low frequency (0.46 kHz) and high frequency (4.6 kHz) to evaluate the significance of ultrafine (<0.03 μm) superparamagnetic (SP) ferrimagnetic minerals. Theoretical analysis shows that grains <30 nm in size have contrasting susceptibilities at frequencies of 0.45 and 4.5 kHz (Dearing et al., 1996) whereas grains >30 nm in size show no difference. When lower susceptibilities are observed at higher frequencies they indicate the presence of SP grains because these grains oscillate at low frequencies but are unable to follow high frequency changes and keep in phase with the field. The percentage frequency dependant susceptibility ($\kappa_{fd\%}$) is a measure of the percentage difference between the readings at high and low frequencies where $\kappa_{fd\%} = \{(\kappa_{lf} - \kappa_{hf})/\kappa_{lf}\} \times 100$. κ_{lf} is the corrected reading at low frequency and κ_{hf} is the corrected reading at high frequency. For a $\kappa_{fd\%}$ value <5%, single-domain and multi-domain grains are dominant. For a value >5%, SP grains dominate.

The majority of samples from fissures 1 and 2 have $\kappa_{fd\%}$ values less than 5% (Figs. 6 and 7) and therefore show a dominance of SD and/or MD grains with small contribution from SP grain sizes. No systematic changes in $\kappa_{fd\%}$ with time are evident in these data

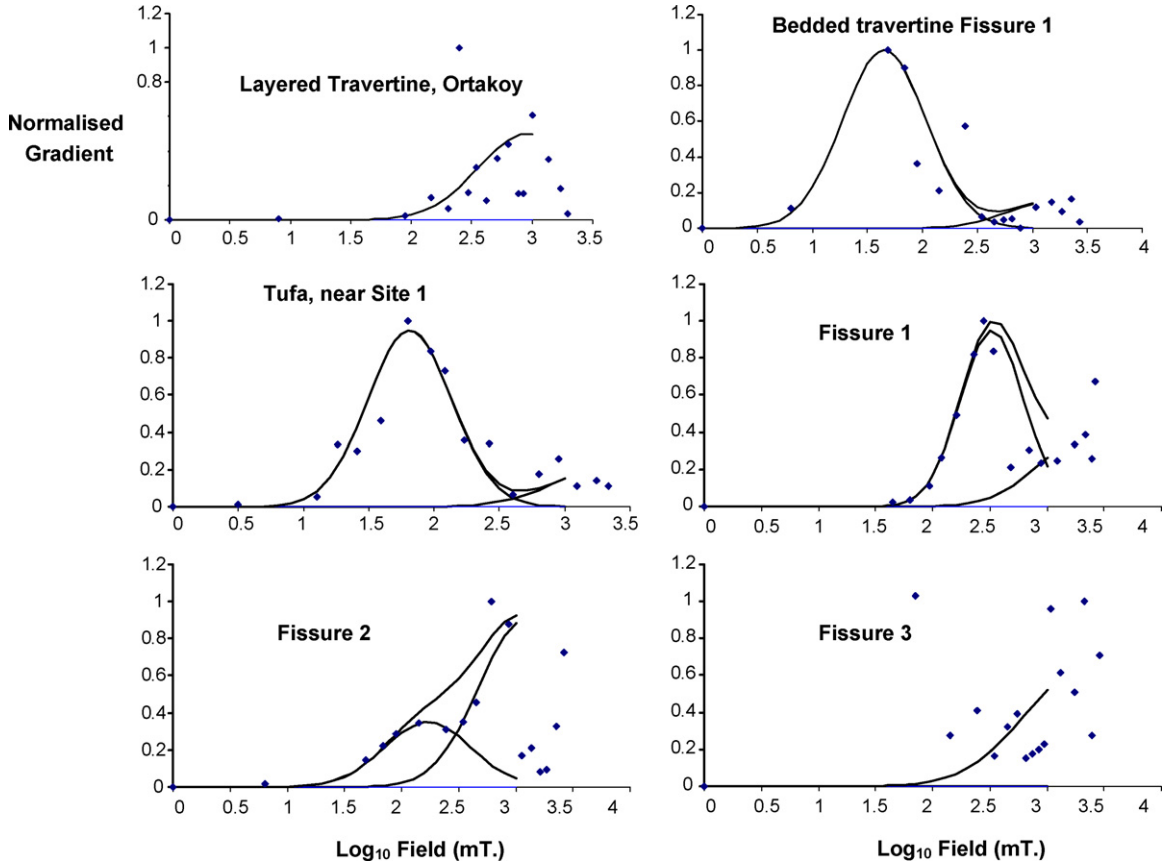

Fig. 5. Representative Isothermal Remanent Magnetisation (IRM) spectra from fissure and bedded travertine analysed following the approach of Robertson and France (1994) by plotting the normalised gradient of the IRM curve against the logarithm of the magnetising field.

although a comparison with $\kappa_{fd\%}$ values measured in bedded travertine from this geothermal field shows that the latter tend to be dominated by SP grains (Fig. 8). This may reflect the input of fine atmospheric dust into the surface travertine during precipitation, although magnetite precipitation from bacterial complexes flourishing in this warm fluid-rich surface environment could also contribute (Chang and Kirschvink, 1989). This contrast in ferromagnetic grain sizes is a function of the contrasting energies of the two environments: in the fissures the hydrothermal waters are pulsed forcibly upwards and able to carry larger particles before they become fixed by carbonate precipitation at the walls, whereas at the surface the waters trickle out over the carbonate mound following loss of the detrital particles in the groundwater.

Access to airborne dust will also contribute ferromagnetic grains to the bedded travertine to produce stronger magnetic properties than in the fissure travertine. In the fissures deposition is restricted to particulate ferromagnets comprising goethite and hematite carried down in meteoric waters from the weathered profile. The bedded travertine in this area is indeed found to be somewhat more strongly magnetised: intensities of magnetisation in 27 measured tufa samples from the vicinity of Fissure 1 range from 0.007 to 0.114×10^{-5} A m^2/kg with a $\log_{10}$ normalised mean of 0.012×10^{-5} A m^2/kg compares with the fissure samples where intensity ranges from 0.001 to 0.168×10^{-5} A m^2/kg with a normalised mean of 0.006×10^{-5} A m^2/kg. Since the tufa has a friable texture and is appreciably less dense than the fissure travertine, this represents a significant difference. The bedded travertines at Ortaköy also have a mean intensity of $0.035 \pm 0.016 \times 10^{-5}$ A m^2/kg which compares with a lower mean intensity of magnetisation of 0.012 ± 0.06 A m^2/kg in Fissure 3. This difference is not ubiquitous; our field observations measuring susceptibility with hand-held kappameter in the Pammukalle travertine of western Turkey identify stronger magnetisations in fissure material and suggest that local conditions and source materials are responsible for regional variations.

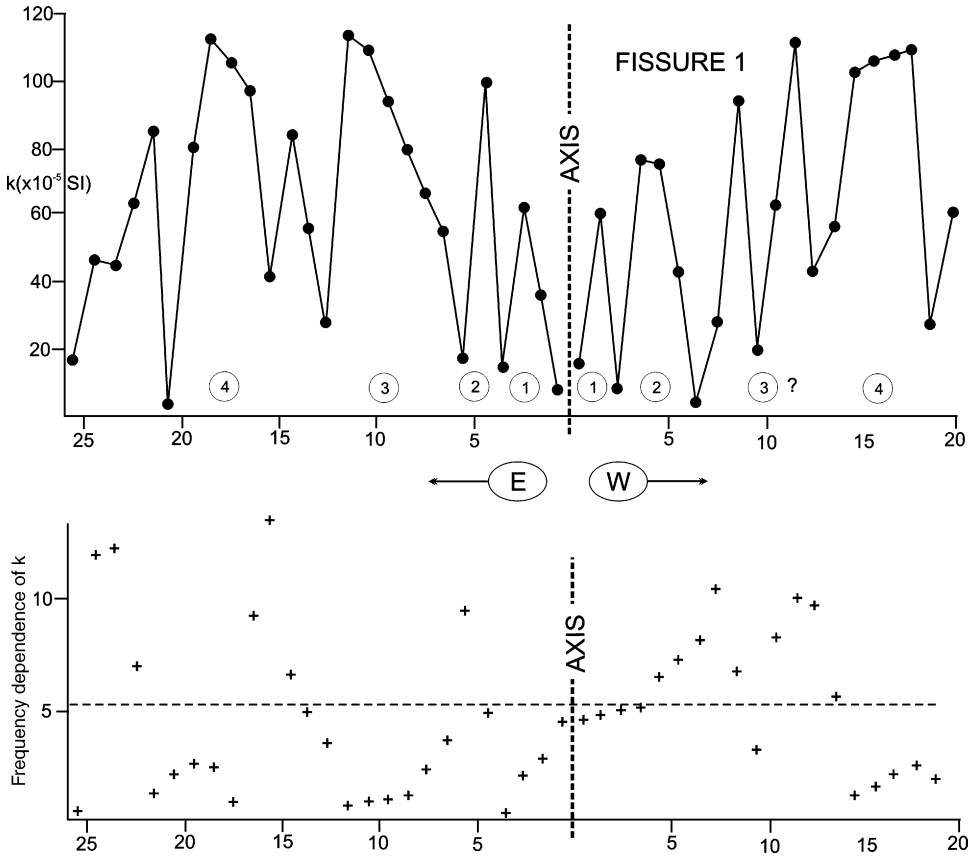

Fig. 6. The variation of magnetic susceptibility (k) and the frequency dependency of susceptibility (κ_{fd}) across travertine Fissure 1. Although the data are plotted as a function of sample number, this is also an approximate distance scale with each group of 10 samples spanning ~30 cm. The circled numbers refer to significant distinctive colour bands enabling the correlation of the sequence on either side of the axis (see also Fig. 3).

5. Magnetic susceptibility and carbonate diagenesis

X-ray diffraction studies conducted on samples from Fissure 1 aimed to clarify magnetic mineralogy but had only limited success in resolving the ferromagnets identified from palaeomagnetic study (Section 7), probably because the latter occur as dispersed particles. A goethite peak was detectable in all 12 examples and was the dominant peak in eight; a minor hematite peak was present in four samples beyond core 9. The aluminium oxide boehmite (AlO(OH)), a product of weathering of aluminium silicates in warm temperate and tropical climates, is detectable in 8 examples and becomes more important than goethite near the axis as magnetic susceptibilities diminish (Fig. 6).

The mineralogy of the dominant carbonate $CaCO_3$ was also determined in all samples from travertine at Fissure 1 and correlates positively with magnetic susceptibility (Fig. 9): the more magnetically susceptible samples are those dominated by calcite, whereas samples dominated by aragonite tend to be weakly magnetic. The precipitation of calcium carbonate as aragonite is considered to depend on the Mg^{2+} concentration as well as on the partial pressure of CO_2 between the solution and the atmosphere (Duchi et al., 1978). The relationship to Fe^{2+} and Fe^{3+} concentrations does not yet appear to have been investigated, but in bedded travertine dissolution and reprecipitation processes by meteoric waters rapidly convert aragonite to calcite (Turi, 1986) and the ratio between the two is a strong positive signature of diagenesis. However, unlike layered travertines which tend to be open textured and permeable, fissure travertine is massive and impervious crystalline material which quickly becomes sealed from the hydrothermal system. We therefore suspect that the calcite to aragonite variations observed in Fissure 1, paralleled by the changes in magnetic susceptibility in this example, reflect long-term changes in the chemistry and CO_2 partial pressures within the hydrothermal reservoir.

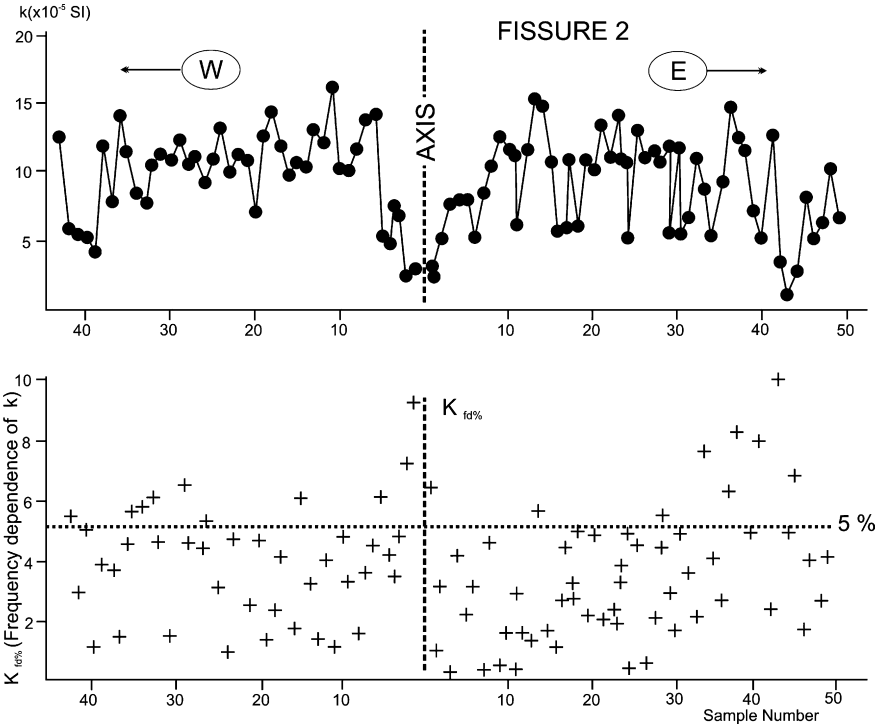

Fig. 7. The variation of magnetic susceptibility (k) and the frequency dependency of susceptibility (κ_{fd}) across travertine Fissure 2.

6. Magnetic fabrics

Anisotropy of magnetic susceptibility (AMS) is present when grains have been aligned during deposition by a mechanism such as current flow. To evaluate this property in travertine, AMS has been determined on well-shaped cores from fissures 1 and 2, and the bedded travertine collection from Ortaköy using Kappabridge KL-3 delineator. The variation of susceptibility with direction is represented by a 3-3 symmetric tensor and is approximated visually by a triaxial ellipsoid. The principal directions of the ellipsoid are denoted k_1 or $k_{max} > k_2$ or $k_{int} > k_3$ or k_{min}. The degree of anisotropy (P) is defined by k_{max}/k_{min}; lineation (L) is defined by k_{max}/k_{int} and foliation (F) by k_{int}/k_{min}. When $F > L$ the ellipsoid is oblate and when $L > F$ the ellipsoid is prolate in form.

The degree of AMS is found to be much stronger in fissure travertine than in layered travertine and ellipsoid shapes in the fissures are strongly lineated (Figs. 10 and 11). Only one core in Fissure 1 and two cores in Fissure 2 showed marginal prolate fabrics; all the remainder were distinctly, and sometimes strongly, prolate. In contrast, the ellipsoids in the bedded travertine are near neutral with low degrees of anisotropy. The direction of k_{max} in the fissures is horizontal and conforms closely to the trends of the fissure axes; k_{int} and k_{min} are not individually grouped but comprise a girdle oriented at right angles to the plane of the fissure (Fig. 12). The exception is the massive portions of travertine in Fissure 2 which exhibits weak random fabrics in contrast to the layered parts of the same fissure, and data from these cores are excluded from the directional analysis. Both the probable causative ferromagnetic minerals

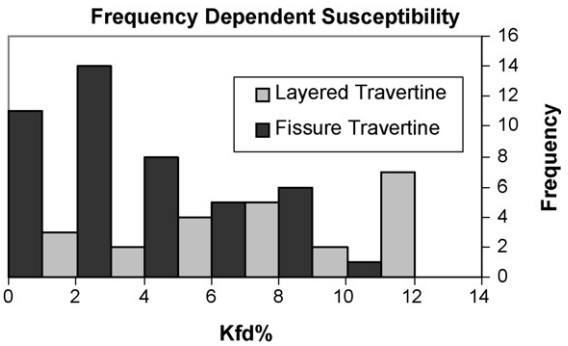

Fig. 8. Comparison of $\kappa_{fd\%}$ values in fissure travertine from fissure locality 1 with values from 23 samples of bedded travertine (sites 4 and 5) in the same geothermal field.

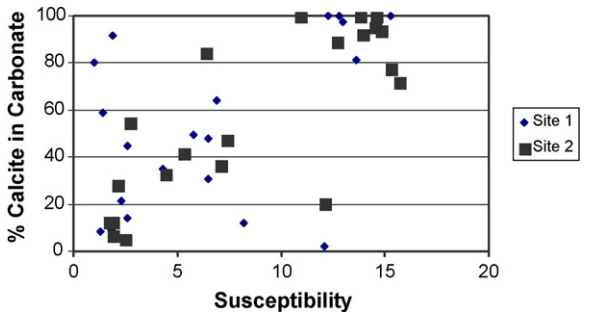

Fig. 9. Calcite/aragonite ratios in the palaeomagnetic cores from Fissure 1 plotted against susceptibility in SI units $\times 10^{-5}$. Sites 1 and 2 embrace samples on the west and east sides of the axis, respectively.

(goethite which is orthorhombic and hematite which is hexagonal) have crystalline anisotropy. However, the strongly lineated nature of the fabric aligned with the dyke axes implies that shape anisotropy is the cause of this effect. Of the four forces controlling the end position of deposited grains (thermal, magnetic, gravity, hydraulic), only hydraulic and gravity could operate to produce the observed horizontal alignment of k_{max} in the plane of the fissure. As observed in stream channel flow, elongate particles are oriented by hydraulic currents with their long axes perpendicular to the direction of flow, which in this case is vertically up the fissure. Larger grains may be expected to roll back down the walls of the fissure after each ejecting steam-forced pulse until they become fixed by the carbonate precipitation thus also accounting for the girdle distribution of k_{int} and k_{min}. The only prominent alignment of susceptibility axes in the bedded travertine is a tendency for k_{min} to be perpendicular to the plane of the ground (Fig. 12). This is most readily explained in terms of a shape effect as particles with more oblate shapes settle out of the water into the plane of the ground. The particles in this case will be suspended or rolled at low velocities by waters moving over the surface of the travertine mound and deposited as hydraulic flow fails and grains become aligned into the magnetic field by a process analogous to post-depositional remanent magnetisation. Atmospheric additions will also contribute to the fabric in this case with finer particles highlighted by the $\kappa_{fd\%}$ analysis settling into alignment with the ambient field; if these include magnetite grains, the latter could dominate fabric in bedded travertine due to their much higher susceptibilities.

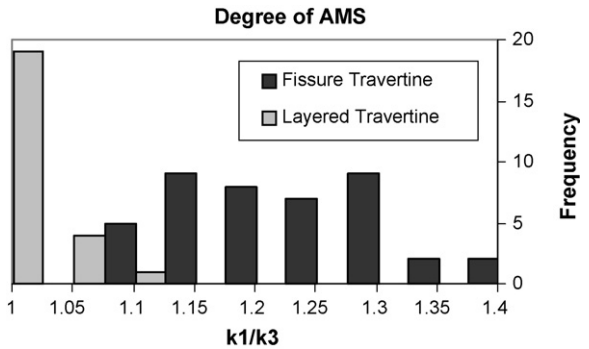

Fig. 10. Histogram comparing the degrees of anisotropy of magnetic susceptibility in fissure and bedded travertine.

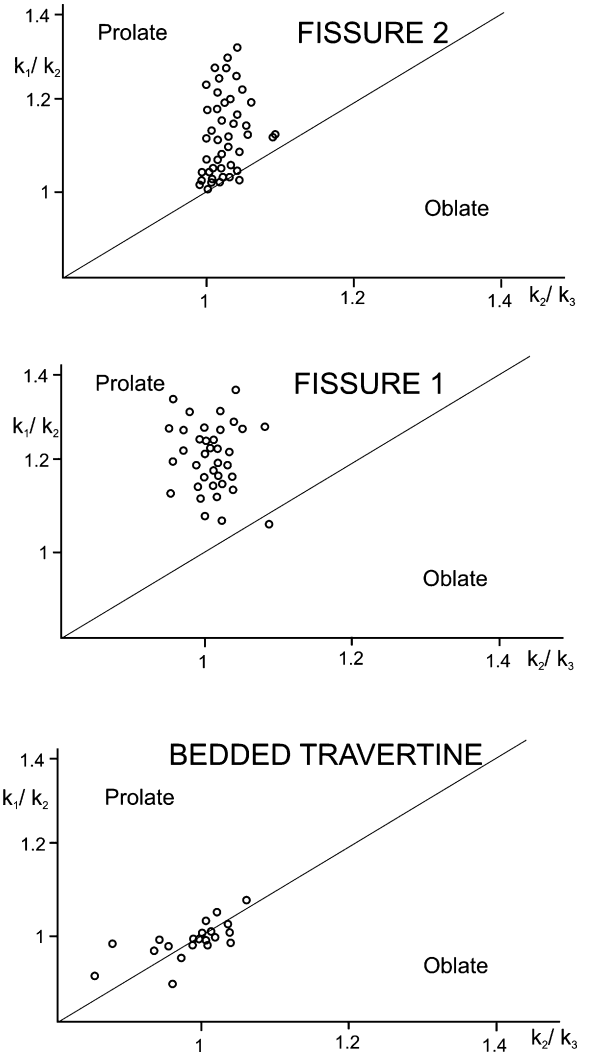

Fig. 11. Lineation of AMS plotted against foliation in travertines Fissures 1 and 2 and bedded travertine from the Ortaköy geothermal field.

7. Palaeomagnetic analysis

Palaeomagnetic cores were treated as noted in Section 3; Fig. 13 illustrates examples of orthogo-

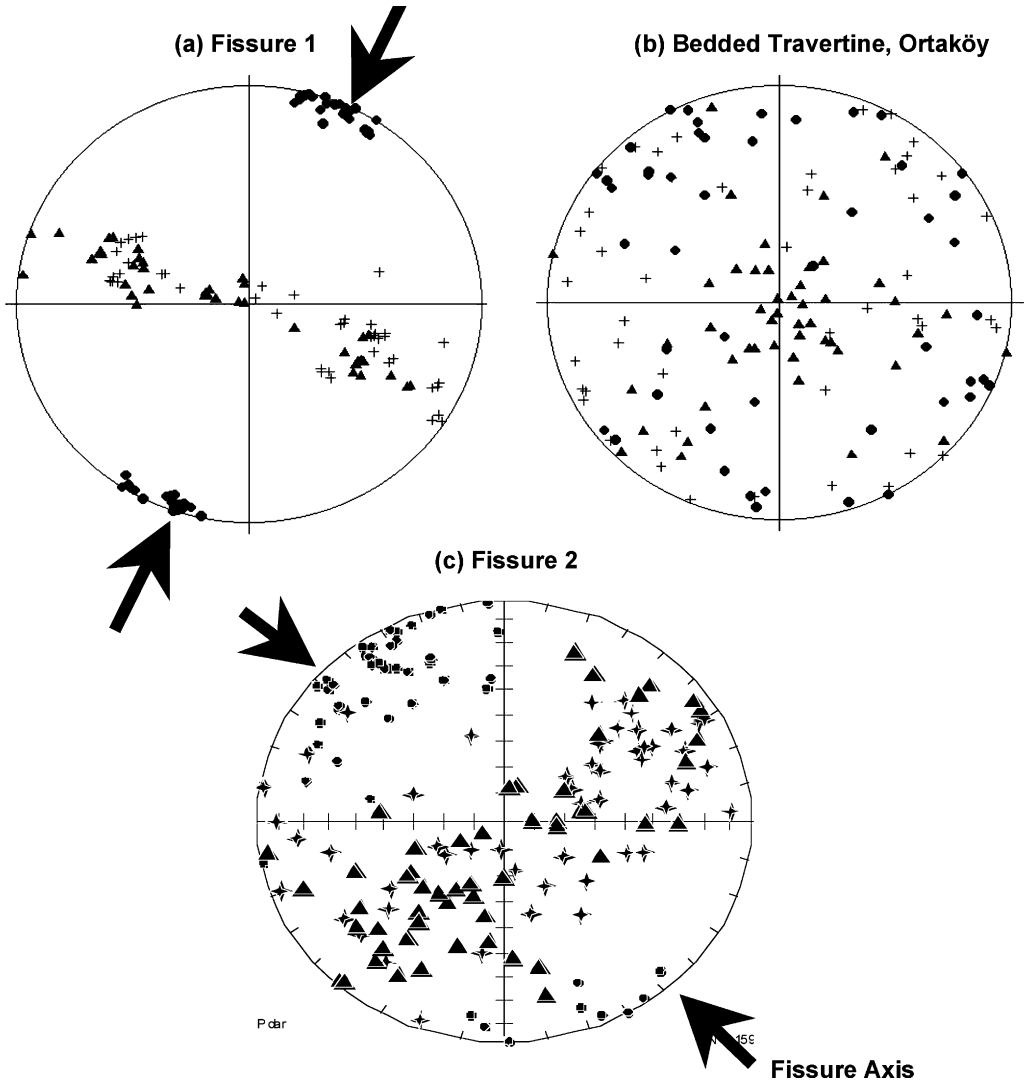

Fig. 12. Directions of maximum, intermediate and minimum susceptibility axes in the fissured travertine at Sıcak Çermik and the layered travertine at Ortaköy. Projections are onto the lower hemisphere of an equal area projection. Note that the maximum susceptibility axes in the fissure travertine correlates with the trend of the extensional fissure axes (arrows). Circles are the directions of $k_{maximum}$ axes, crosses are the directions of $k_{intermediate}$ axes and triangles are $k_{minimum}$ axes.

nal projections from the three fissures and the range of bedded travertine. Samples from fissures 1 and 2 and from the bedded travertine at Ortaköy were subjected to a.f. demagnetisation; variable contributions from high coercivity ferromagnets often produced only short trajectories although these could usually be identified as converging. Fissure 3 was subjected to thermal demagnetisation in order to compare the two methods of treatment and evaluate the possible contribution of goethite (Curie point ~125 °C) to the remanence. This treatment could usually be conducted to 300–350 °C before the carbonate host began to disintegrate.

7.1. Fissure locality 1

Fissure 1 is a 2 m wide example yielding U–Th ages of 120 ± 5 year at the axis and $177^{+14}/_{-13}$ ka at the margin (Mesci, 2004); the error limits on these age determinations are analytical and cannot be taken as real indications of age uncertainty. Fig. 1 shows the location and Fig. 3 illustrates the sample distribution comprising 23 samples to the right of the axis (Site 1, W) and 26 samples to the left (Site 2, E); the distinctively coloured bands permit contemporaneous layers to be matched up on either side of the fissure axis and hence help to validate direc-

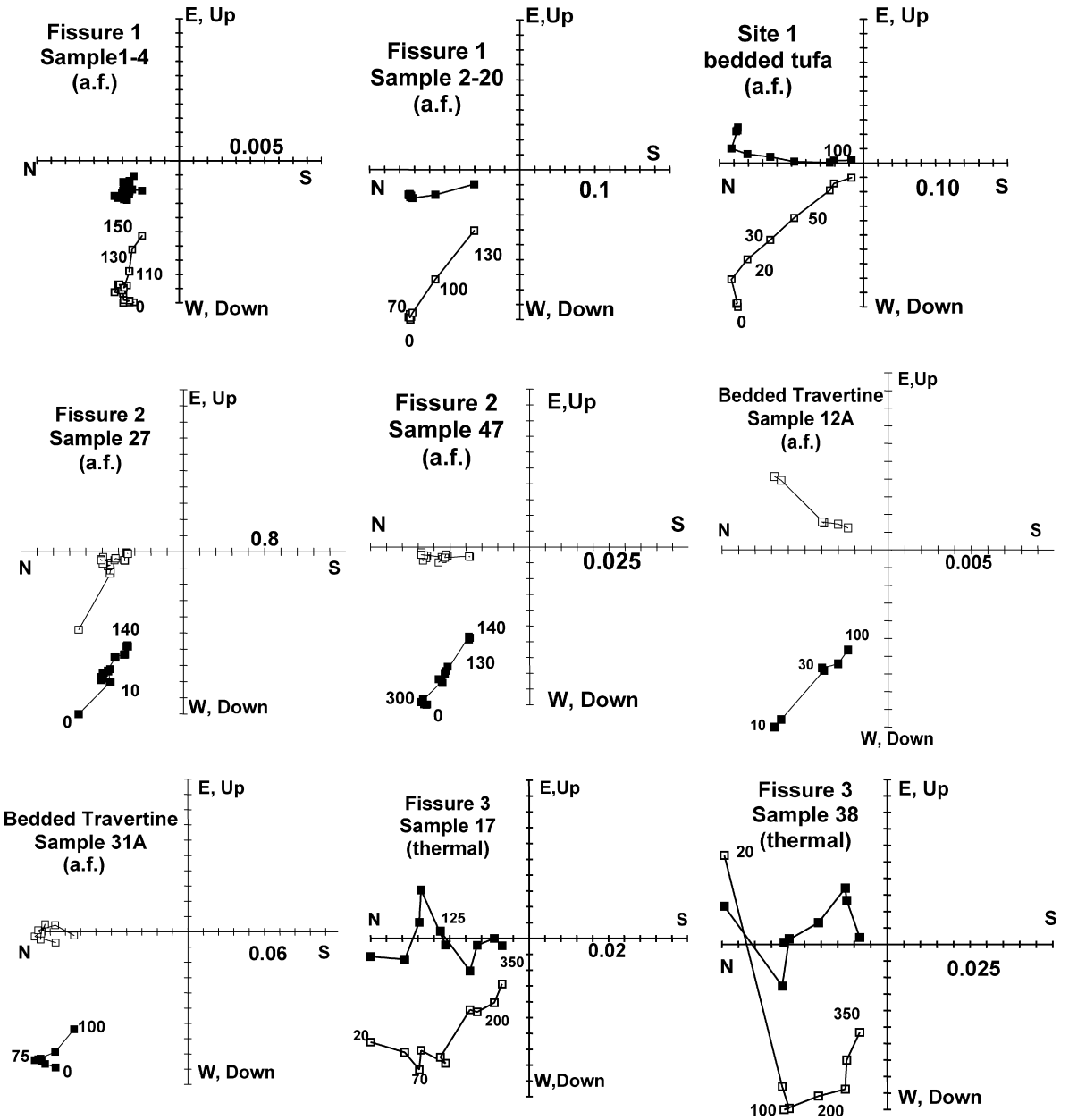

Fig. 13. Orthogonal projections showing demagnetisation behaviours of the fissure and bedded travertine studied here. Projections of the magnetisation vector onto the horizontal plane are shown as the closed symbols and projections onto the vertical plane are shown as the open symbols. Fields of treatment are in milliTesla (mT) and °C in the case of the travertine examples from Fissure 3. The intensity values are $\times 10^{-5}$ A m^2/kg.

tional changes across the fissure. The travertine has weak but measurable remanence following a.f. demagnetisation; components defining directions with mean angular deviations of $\leq 25^\circ$ were considered meaningful and accepted. To minimise uncertainties introduced by individual cores successive mean directions of magnetisation were calculated from threefold running means to evaluate directional trends across the fissure; the typical influence of this procedure is illustrated in Figs. 17 and 18.

Magnetic declinations on the left and right hand sides of the fissure show similar variation with a swing of the palaeofield initially to the east, then to the west, and lastly back to the east (indicated as cycles 1 and 2 in Fig. 14). The inclination records also correspond very closely out to sample 12 but beyond this point they diverge with site 1

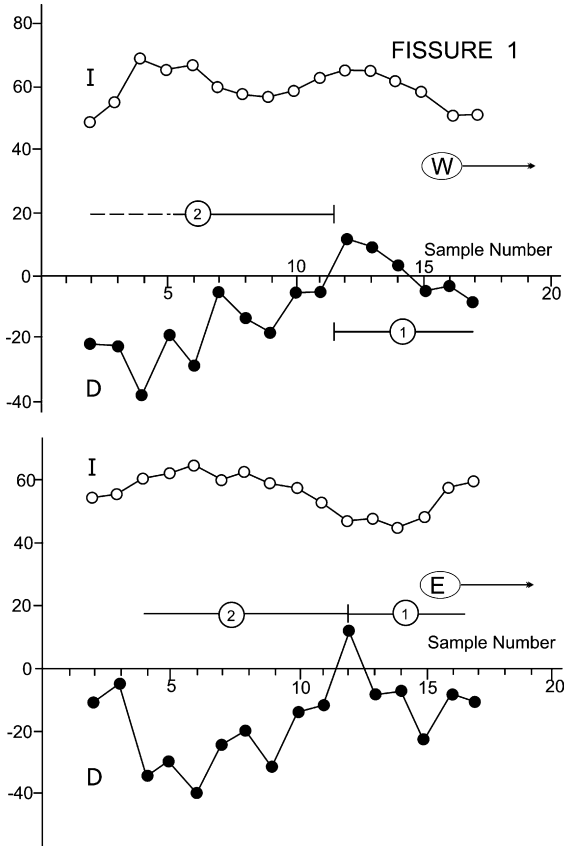

Fig. 14. Variation in the declination and inclination of the magnetisation on each side of the axis of Fissure 1.

becoming steeper and site 2 shallower than the mean field inclination in this region. The variation in declination is of higher frequency than the variation in inclination, an observation that emerges from the historical PSV record in Europe (e.g. Marton, 1996). The mean direction yielded by the running means of the samples from site 1 on the west side of the fissure axis is $D/I = 348.7/58.7^\circ$ ($N = 18$, $R = 17.21$, $\alpha_{95} = 7.6^\circ$, $k = 21.5$) and from site 2 on the east side of the axis is $D/I = 345.2/56.0^\circ$ ($N = 18$, $R = 16.93$, $\alpha_{95} = 8.9^\circ$, $k = 15.9$). These declinations are rotated clockwise in common with most late Tertiary rocks of central-east Anatolia (Piper et al., 2006) but inclinations are not significantly shallower than the inclination predicted from the geocentric axial dipole field at the sample locality ($I = 59^\circ$). Beyond sample 18 (Fig. 3) it is not possible to correlate bands on either side with confidence and beyond core 21 in site 1 the layering is truncated at the base of the outcrop with older layers recording a separate period of growth.

Some 60 cm of travertine growth at this locality thus appear to be just short of recording a complete cycle of secular variation. Analogies with the historical field and the lake sediment record (Butler, 1992) suggest that some 2000 years of deposition are likely to be represented and suggest a rate of carbonate incrementation of ~0.3 mm/year. Approximately 50 individual layers are discernible within this thickness implying that earthquakes large and/or close enough to reset the reservoir and stimulate water flow occurred roughly every 40 years. At this locality the record of PSV thus indicates a fissure lifespan much shorter than the 177,000–120,000 year interval suggested by the U–Th evidence, a point that we address below in the context of the data from fissures 2 and 3.

7.2. Fissure locality 2

This is a ~3 m wide fissure dated by U–Th at $271^{+64}/_{-42}$ ka at the axis and $299^{+37}/_{-29}$ ka at the margin. The palaeomagnetic sample comprises 49 samples from the east side (site 3) and 43 samples from the west side (site 4). Samples were subjected to a.f. demagnetisation incremented in steps of 5–35 mT and then in fields of 50, 75, 100 and 140 mT. All samples were characterised by high magnetic coercivities although treatment was usually able to subtract sufficient remanence to demonstrate convergent vectors and identify single component behaviours (Fig. 13). Component directions fall into two groups: the majority of components show directions close to the present field with small consecutive directional change between adjacent cores (Table 1). The remainder show directions diverging widely from the Recent field direction although approximately consistent between adjacent cores until there is a shift to the predicted field direction (Table 1). The outer parts of this fissure beyond core 27 show thin parallel layers of travertine that are readily correlated on either side. Comparable swings in declination and inclination can be identified in this part of the fissure (sequence 1 in Fig. 15) and suggest that one full cycle of PSV is recorded within this initial (outer) sequence of travertine deposition: only fragments of a subsequent cycle are recorded although the last pulse of deposition appears to have recorded approximately a half a cycle before the fissure became extinct (cycle 3 in Fig. 15). The initial phase of layered travertine (about 1.5 cycles of PSV) records 31 layers of travertine whilst the last (half cycle) records 8 layers. In each case the deposition of one travertine layer in roughly 100 years is indicated with travertine deposition taking place at a rate of approximately 0.2 mm/year.

Thirty eight of 47 samples from site 3 (east) having directions comparable with the Recent field yield a mean direction of $D/I = 339.8/60.3^\circ$ ($\alpha_{95} = 3.9^\circ$) and 28 of 42 samples from site 4 (west) have a mean of

Table 1
Summary of Palaeomagnetic directions from travertine samples in Fissure 2 from the Sıcak Çermik geothermal field, Central Turkey

Site 3 (east)	*D*	*I*	Site 4 (west)	*D*	*I*
2[a]	133.3	41.6	2[a]	75.1	8.0
3[a]	135.6	34.5	3	17.2	23.6
4[a]	148.7	32.8	4	353.5	29.4
5[a]	157.5	25.2	5	358.2	42.2
6	343.7	63.9	6	358.2	42.2
7	321.2	74.6	7	353.8	66.2
8[a]	147.3	70.8	8	334.7	77.8
9[a]	162.4	72.7	9	321.3	68.0
10[a]	131.8	83.2	10	336.8	56.4
11[a]	268.2	82.9	11	346.6	52.4
12	326.4	73.3	12[a]	168.4	21.0
13	326.8	67.4	13	338.0	46.1
14	330.0	55.5	14[a]	153.8	31.3
15[a]	232.0	26.5	15[a]	144.0	27.7
16[a]	203.3	44.1	16[a]	127.3	45.1
17	325.2	67.2	17[a]	137.1	42.2
18	311.4	57.1	18[a]	127.2	51.7
19	324.3	51.1	19[a]	49.8	34.2
20	329.1	56.6	20[a]	64.8	49.2
21	333.4	58.6	21[a]	112.6	59.4
22	323.2	58.0	22[a]	130.3	52.4
23	335.3	51.7	23	338.5	58.5
24[a]	186.4	-13.6	24	341.3	62.1
25	14.0	63.6	25	343.7	66.5
26[a]	144.8	59.3	26[a]	190.8	33.8
27	2.6	68.2	27[a]	243.0	20.2
28	2.6	60.3	28	357.7	70.0
29	356.1	54.7	29	356.9	68.0
30	354.4	61.6	30	6.3	62.9
31	338.8	64.1	31	2.9	59.0
32	338.0	56.8	32	10.8	62.3
33	325.0	54.5	33	14.1	63.5
34	317.4	53.7	34	8.8	65.8
35	315.1	57.3	35	1.2	64.0
36	335.0	59.8	36	358.5	61.8
37	346.9	62.1	37	352.0	58.5
38	353.4	64.6	38	340.6	56.9
39	348.8	63.9	39	346.2	57.7
40	349.9	61.2	40	352.8	61.7
41	344.4	61.1	41	354.6	61.3
42	347.7	60.3	42	358.9	69.2
43	334.3	62.1			
44	333.1	63.4			
45	349.7	60.1			
46	359.7	55.9			
47	0.9	52.2			
Mean result, Site 3, East side of fissure:					
	338.8	61.43		N/R = 34/33.54, $\alpha_{95} = 2.9^\circ$, $k = 72.0$	
Mean result, Site 4, West side of fissure:					
	355.2	58.7		*N*/*R* = 28/27.23, $\alpha_{95} = 4.7^\circ$, $k = 35.2$	

N is the number of samples and *R* is the magnitude of the resultant vector. α_{95} is the radius of the cone of 95% confidence about the mean direction and *k* is the Fisher precision parameter (=$(N-1)/(N-R)$).

[a] Samples yielding anomalous directions of magnetisation; these correlate mostly, but not exclusively, with non-layered (massive) travertine.

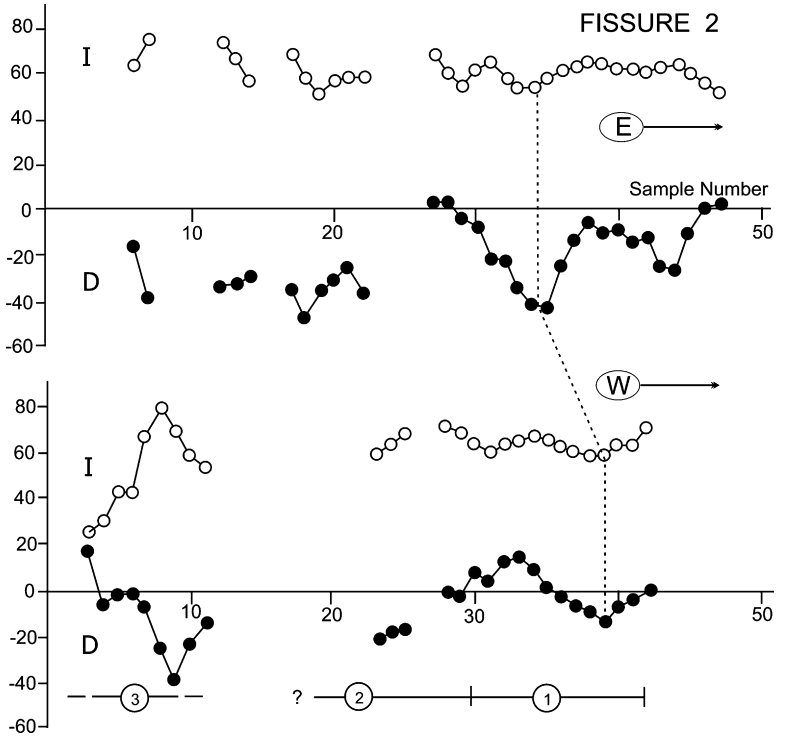

Fig. 15. Variation of the magnetic declination and inclination recorded by travertine growth across Fissure 2. The travertine axis is on the left hand side and samples increase in age to the right. The circled numbers indicate cycles of inferred PSV.

$D/I = 356.8/60.3^\circ$ ($\alpha_{95} = 5.8^\circ$). Thus as in Fissure 1, the recorded geomagnetic field is rotated anticlockwise but the inclination is not significantly removed from the geocentric dipole value of 59°.

The segment of this fissure which failed to yield palaeomagnetic directions comparable with the ambient field direction correlates with the presence of distinctive travertine (Fig. 16). In this segment the banding either has contorted shapes or is massive (i.e. without visible layering) and the predicted field is only incidentally recorded. It appears that precipitation processes within the fissure during turbulent flow or incidental catastrophic emplacement were inimical to the recording of an ambient field direction (Table 1) and this kind of travertine would therefore appear to be unsuitable for investigating PSV. Due to the insertion of this massive travertine we are unable to estimate the duration of activity in this fissure but on the assumption that it spanned ~3 cycles of PSV (Fig. 15), it could be of the order of 5000 years which is within the margins of error of the U–Th age determinations from the margin and axis noted above. Between 60 and 65 bands are discernible (uncertainties arise due to local truncation) between the axis and the outer core suggesting that resetting of the reservoir by earthquake activity occurred approximately every 80 years. The average carbonate incrementation of the ~145 cm of travertine sampled on each side of the fissure is ~0.3 mm/year although this figure is biased by the massive travertine layer and a more realistic estimate for the rate of growth of the banded travertine is the figure of 0.2 mm/year derived from the initial phase of deposition.

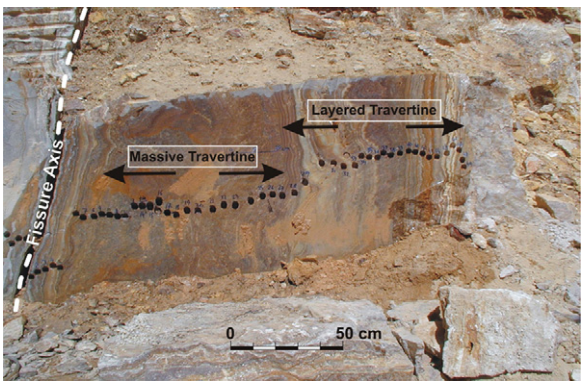

Fig. 16. Photograph of Fissure 2 (eastern side) showing the distribution of palaeomagnetic samples and contrasting types of fissure travertine. The latter comprise uniformly layered travertine, convolute layered travertine and massive (non-layered) travertine.

7.3. Fissure locality 3

This is a wide fissure dated by U–Th analysis as 123 ± 9 ka at the axis and $364^{+201}/_{-76}$ ka at the margins (Mesci, 2004). It is the widest fissure investigated here although it was cored on one side only so we are unable to compare growth on each side of the axis.

Samples were treated by thermal demagnetisation to evaluate the use of this method applied to travertine and determine whether goethite, presumed to be a component of the brown colour, is a significant remanence carrier. Thermal demagnetisation could then surmount the difficulty that magnetic coercivities in travertine are often high and component trajectories correspondingly difficult to define. Since goethite has a Curie point of only ~125 °C, steps of just 25 °C were used commencing at 50 °C and continuing to 150 °C. In the event, only marginal reduction of the remanent intensity of 5–10% had been achieved by this temperature thus showing that hematite rather than goethite must be the carrier of high coercivity remanence identified from a.f. demagnetisation (Fig. 13). Thermal demagnetisation was continued in 50 °C steps until the carbonate began to disintegrate at ~350 °C; this achieved variable reduction in natural remanent magnetisation and often allowed convergent vectors to be recognised and defined.

To illustrate the effect of calculating successive 3 point means to determine palaeofield migration across a fissure we show both the raw and smoothed data for declination in Fig. 17 and inclination in Fig. 18. Continuing to adopt the criteria that a swing in declination and/or inclination is only significant if it is recognised in more than one successive sample, we identify 5 complete cycles of PSV across this fissure. These are evident in both the raw and smoothed data (Figs. 17 and 18) with the chief uncertainty being within cycles 3 and 4 where three counter clockwise swings in declination are observed although the complementary clockwise swing is defined with confidence only in the earlier part of cycle 3. As in Fissures 1 and 2, declination changes are higher in frequency and magnitude than inclination changes. Approximately 85 layers are discernible across this fissure as distinct bands ranging from white through shades of yellow to brown. From the assumption that approximately 10,000 years of travertine growth are recorded here, this indicates that an earthquake large enough to reset the reservoir occurred approximately every 120 years and that the rate of carbonate growth was ~0.1 mm/year on each side of the fissure.

Table 2
Summary of Palaeomagnetic results from bedded travertine deposit at Ortaköy, Central Turkey

Layer number	*D*	*I*	*N*/*R*	α_{95}
1	(348.5)	(49.5)	1/–	
2	5.8	41.1	2/2.00	6.7
3	348.6	50.3	2/2.00	2.2
4	354.6	44.7	2/2.00	10.6
5	359.6	51.6	2/2.00	7.8
6	22.4	53.4	3/2.99	8.3
7	1.6	47.7	2/1.98	32.2
8	6.2	47.2	2/1.98	35.2
9	21.2	36.6	2/1.99	19.2
10	338.0	34.7	2/2.00	9.9
11	346.4	36.2	4/3.96	10.8
12	323.9	33.8	2/1.99	24.5
13	2.6	36.4	2/2.00	3.5
14	327.9	51.8	3/2.94	22.1
15	338.9	40.7	3/2.97	14.6
16	358.8	39.6	2/2.00	13.1
17	349.0	48.1	2/1.99	22.8
18	6.2	48.3	2/1.99	19.7
19	8.9	59.3	2/1.99	24.6
20	–	–	–	–
21	(347.2)	(65.6)	1/–	
22	329.1	51.7	3/2.96	16.9
23	358.0	53.5	3/3.00	4.5
24	352.7	49.1	2/2.00	7.8
Mean result (23 layers)	353.5	47.6	23/22.40	5.1

N is the number of samples and *R* is the magnitude of the resultant vector. α_{95} is the radius of the cone of 95% confidence about the mean direction. Directions in brackets are derived from single samples.

7.4. Bedded travertine (ortaköy geothermal field)

A comparative sample of bedded travertine has been collected from the Ortaköy Geothermal field located SW of Sıcak Çermik and comprises 24 successive layers derived from a single travertine mound. The basal layer overlies volcanoclastic sediments and a 2 m thick basal layer of massive and brecciated travertine. Succeeding layers range from 14 to 50 cm in thickness and comprise a total thickness of 7.9 m to the summit of the mound. This deposit is undated although geothermal activity is present nearby and it seems likely to be several tens of thousands of years old. Two samples were drilled from each layer and used to derive layer means with 95% confidence limits summarised in Table 2.

Mean declinations and inclinations are summarised as a log in Fig. 19 and compared with a magnetic susceptibility through the same section. All but two layers (8 and 20) yield measurable and stable components of magnetisation, although only single samples in layers 1 and 21 yielded useful data. Layer mean directions are summarised in Table 2 and show typical normal polarity

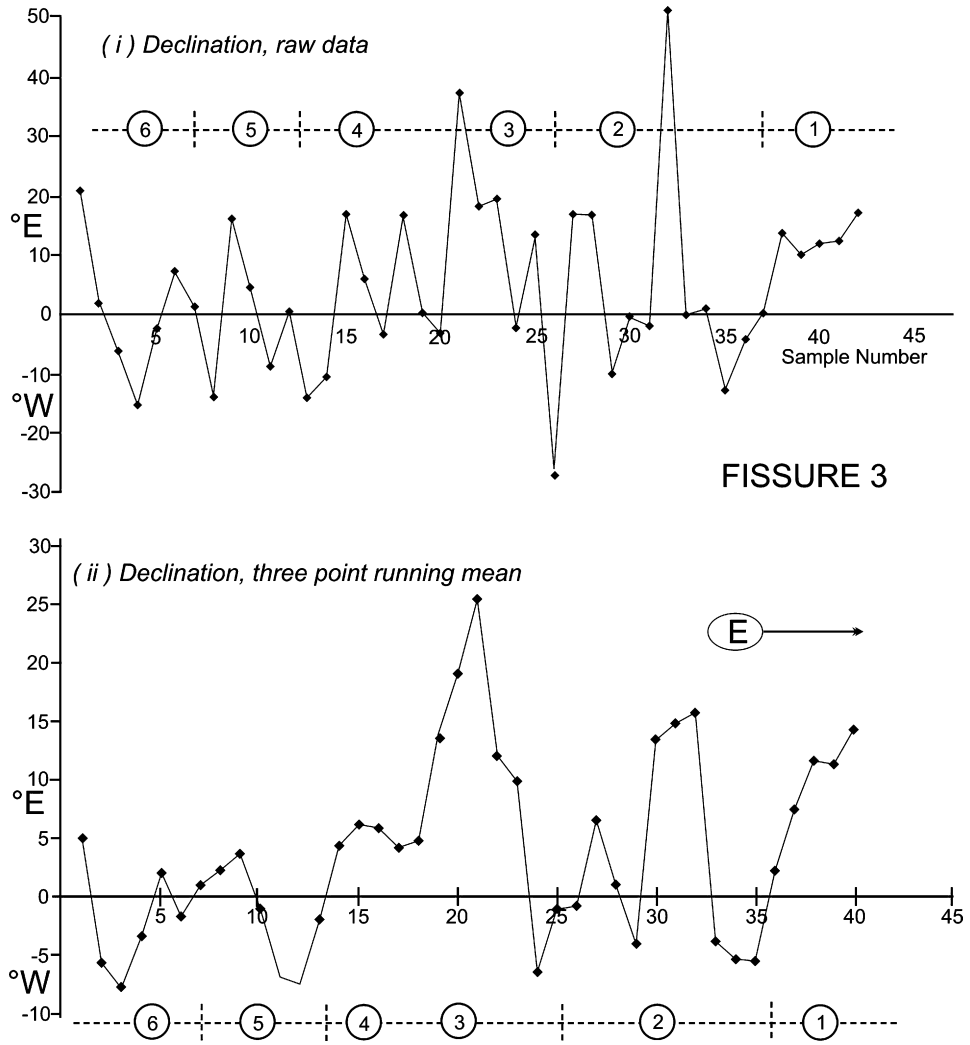

Fig. 17. Variation of the magnetic declination recorded by travertine growth across Fissure 3. Both raw data and Fisherian means derived from applying a three-point overlapping filter are shown. The circled numbers indicate interpreted cycles of PSV.

directions ranging from 324°E to 22°E and inclinations ranging from 35° to 66°. The mean direction derived from 20 layers is $D/I = 354/48°$ and the inclination in this travertine is significantly shallower than the inclination (58.5°) predicted from a geocentric axial dipole source at this latitude (39.4°N). Since no shallowing of inclination is observed in the fissure travertine, a depositional mechanism operating in the absence of forced hydrothermal pumping is presumably responsible for this effect in the bedded material.

Since these are bedded travertine which is inherently permeable, it is also possible that diagenesis and remagnetisation could have occurred and render the palaeomagnetic record an imperfect record of the prevailing field. However, excluding declination and inclination swings defined by single layers only, there are systematic changes in direction defined by three or more successive layers and two complete cycles of PSV may be recorded by this log (1 and 2 in Fig. 19) and imply that some 2000–4000 years of deposition are represented with each layer (and equivalent earthquake cycle) recording intervals of the order of 100–200 years. Deposition rates of the travertine would then have been 2–4 mm/year, or about an order higher than the rate of deposition of the layered travertine. This is explained by three effects: (i) the carbonate-charged water is preferentially blown forcibly out of the fissure by activity of the steam, (ii) the largest reduction in PCO_2 takes place at the surface and (iii) it is here that the water moves away only slowly whilst being subject to strong evaporation.

Of especial interest is the large increase in magnetic susceptibility observed between layers 11 and 15

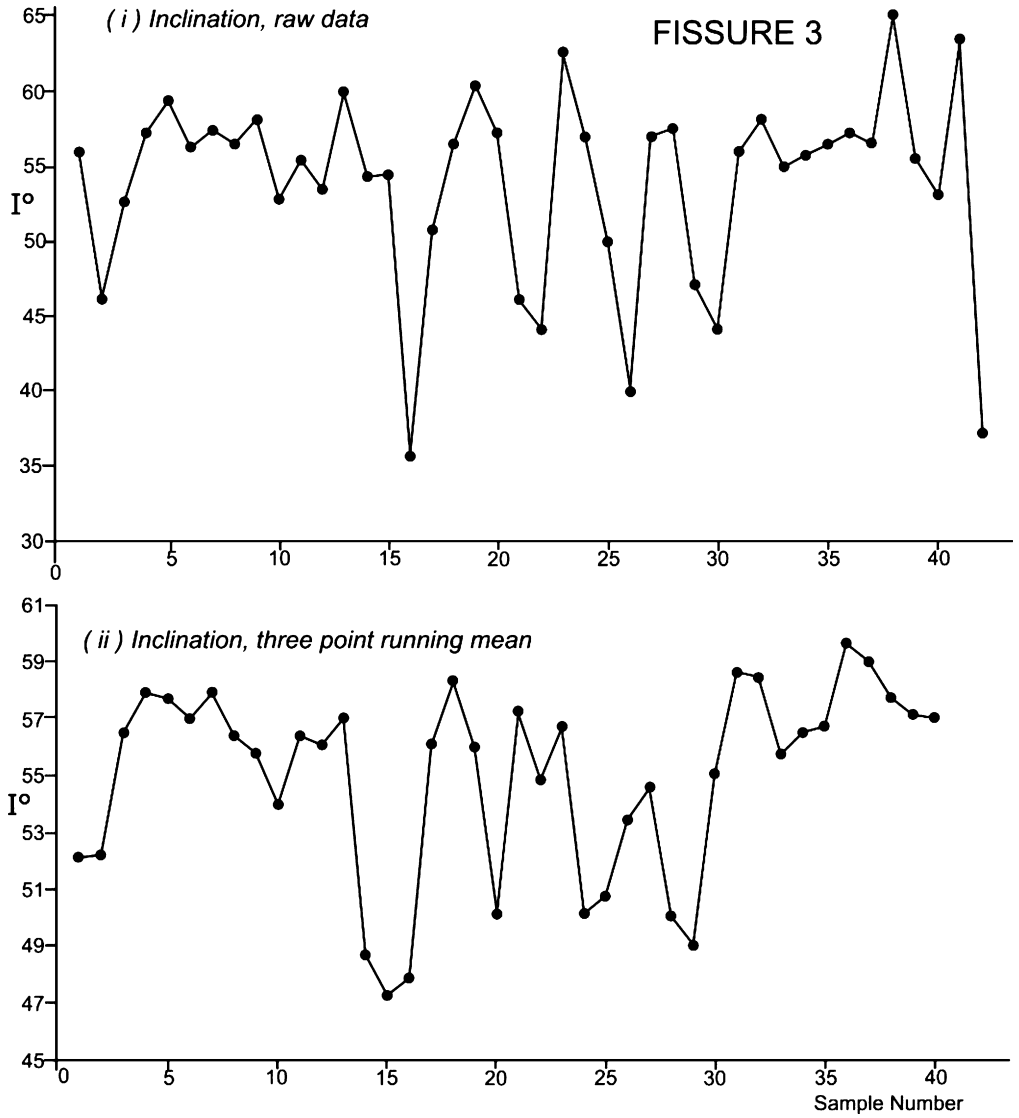

Fig. 18. Variation of the magnetic inclination recorded by travertine growth across Fissure 3. Raw data and Fisherian means derived from applying a three-point overlapping filter are shown for comparison.

(Fig. 19). The dramatic input of magnetic material at this point could have several possible explanations including (i) the signature of a regional volcanic event, (ii) a change in groundwater chemistry, or (iii) a change in the principal wind direction carrying enhanced magnetic detritus into the region. Since the increase in susceptibility is recognised through three successive layers the time period involved is likely to have been several hundreds of years and explanations (ii) or (iii) are therefore more likely. Volcanic outcrops are extensively exposed in the immediate vicinity of Ortaköy and potential sources of wind-borne hematite and magnetite.

8. Neotectonic application

Tectonically controlled travertine is emplaced in actively deforming terranes and the remanence directions are therefore also a signature of rotation about horizontal and/or vertical axes. The Sıcak Çermik geothermal field is sited within the Sivas Basin, a zone of ongoing neotectonic deformation since the closure of the Neo-Tethys Ocean as the Arabian Plate has continued to move northwards into the complex of Anatolian accretionary terranes (Şengör and Yılmaz, 1981). The regional consequence of this deformation is the westward extrusion of terranes (tectonic escape) which

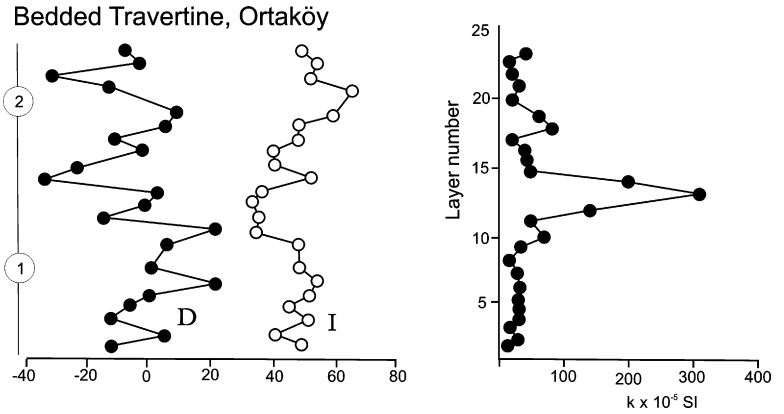

Fig. 19. Variation of magnetic declination and inclination derived from palaeomagnetic study of 24 successive layers through bedded travertine in the Ortaköy geothermal field. Also shown is the variation of magnetic susceptibility through this succession.

appears to be accommodated by multiple differential block movements expressed by regional rotations (Piper et al., 2006); the blocks are delineated by major strike slip faults, although being sites of preferential erosion and basin formation, they are not typically well exposed. Anticlockwise block rotation in the Sivas Basin determined from palaeomagnetic analysis of Pliocene to Pleistocene age lavas is $24 \pm 13^\circ$ (Piper et al., 2006). Constraining this rotation within the last 2–3 Myr is not possible from the volcanic rocks alone where age criteria are mostly morphological and stratigraphic control within the regional terrestrial/lacustrine sediments is poor. Nevertheless, it is clear that this rotation has been concentrated within Plio-Pleistocene times because the rotations determined from older Miocene ($29 \pm 10^\circ$) and Palaeogene ($24 \pm 7^\circ$) rocks are similar. It is therefore considered that rotations associated with tectonic escape have only occurred during the last phase of the neotectonic history following a protracted period of crustal thickening succeeding the closure of Neo-Tethys (Piper et al., 2006).

The recovery of palaeomagnetic directions from travertine dated by U–Th offers the prospect of constraining the timing and rate of young rotation within the latest (Plio-Pleistocene) phase of neotectonic deformation. Sıcak Çermik lies near the centre of a 100 km long belt of geothermal activity trending N40°E and block rotation is hypothesised to occur within a torsional stress system embraced by NE–SW left lateral shear zones (Mesci et al., 2007). This system produces orthogonal compressive and extensional stress fields responsible for travertine growth in shear and tensional fractures, respectively (Fig. 20).

Three of the four travertine units in this study record the anticlockwise rotations characterising the Sivas Basin with magnitudes somewhat less than the mean rotation for the Plio-Pleistocene interval. They collectively imply that the neotectonic rotation has been concentrated within a time period much less than the ~3 Myr embraced by the mean Plio-Pleistocene lava result and has occurred at a rate of the order of ~5°/10,000 years (Fig. 20, inset). This high rate of rotation is similar to block rotation rates identified in the Aegean (Van Hinszberger et al., 2005) and close to the North Anatolian intracontinental transform (Piper et al., 1997). The result from Fissure 3 shows no significant rotation from the present field direction (Table 3) and there are two difficulties with including this result in the tectonic analysis: (i) the errors on one of the age determinations are very large (Section 7.3) and (ii) this result comes from a N–S trending fissure which is not a member of the tension fracture system; it is possibly the youngest fissure investigated here although we are unable to confirm this.

9. Discussion

Although the results of U–Th dating are able to show that geothermal activity in the Sıcak Çermik geothermal field has spanned the last 300,000–400,000 years, they are unable to constrain the intervals of activity within individual fissures with precision; the PSV cycles identified here show that these intervals were significantly shorter than suggested by the U–Th dating. There are some 25 fissures in this geothermal field (Fig. 2) and on the assumption that fluid outflow was concentrated on one fissure at a time, they may have been active for ~12,000 years on average. Although the signature of PSV within the fissures studied here implies activity over significantly shorter intervals than this at fissures 1 and 2, this discrepancy is more apparent than real because the full history of fissure growth is only recorded at the

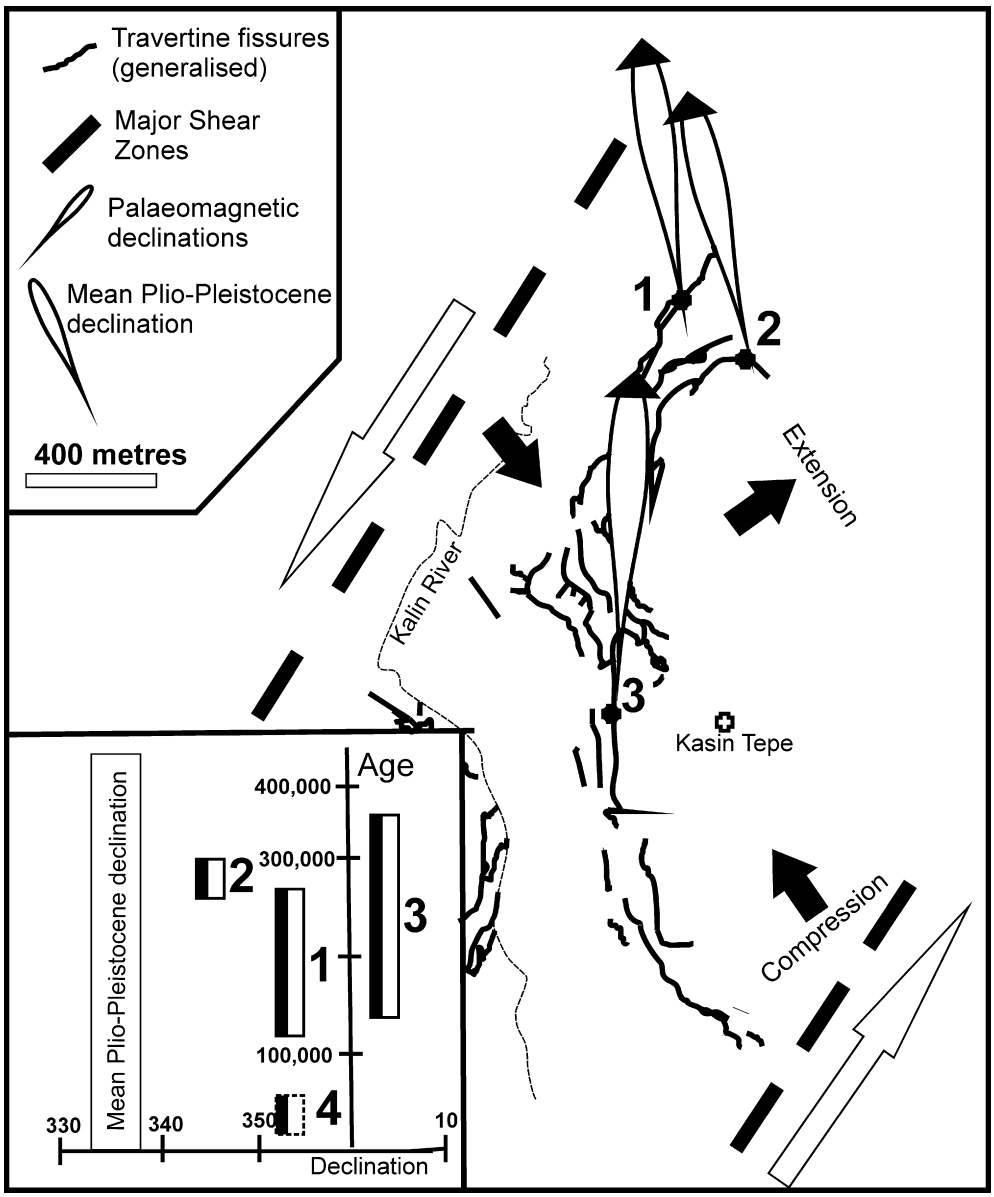

Fig. 20. Mean directions of magnetisation derived from travertine fissures in the Sıcak Çermik geothermal field. Results from fissures 1 and 2 are rotated anticlockwise but by smaller amounts than the mean Pliocene-Pleistocene field direction. The inset graph shows palaeomagnetic directions plotted as a function of ages estimated from U–Th study; the bedded travertine from locality 4 to the south west is assumed to be a few tens of thousands of years old on morphological grounds; a travertine nearby is dated 57.5 ± 2.3 (Mesci et al., 2007).

base of each fissure mound (Fig. 1); as the travertine pile builds up the fissure advances through successive layers so that the highest parts record only the last phase of activity in the fissure. Hence the record of PSV within a fissure will be controlled by the depth of exposure and the level of sampling.

The record of past earthquakes beyond historic and archaeological timescales relies on the identification of catastrophic events in the geological record. Movements along fault planes are the most direct signatures with slickenlines indicating the latest sense of motion and offsets providing the cumulative movement of many successive events. Liquefaction of incompetent sedimentary layers is another feature that provides evidence for ground shaking by earthquake events but in the geological record it cannot usually be constrained within a narrow timeframe and is of little temporal value. The past directional behaviour of the Earth's magnetic field

Table 3
Mean palaeomagnetic directions calculated at sample level from travertine fissures and bedded travertine compared with the mean regional Plio-pleistocene palaeomagnetic geomagnetic field direction for the Sivas Basin

Unit	Age (ka)	*D*	*I*	*N*	*R*	α_{95}	*k*
Fissure 1	120–271	353.7	53.0	38	36.88	4.1	32.9
Fissure 2	271–299	346.0	60.4	62	60.63	2.7	44.4
Fissure 3	123–364	3.4	54.2	41	40.39	2.8	66.0
Bedded travertine	?10–50[a]	353.5	47.6	23	22.40	5.1	46.7
Regional field[b]	Plio-pleistocene	336	47	–	–	13.0	–

[a] Estimated to be a few tens of thousands of years old on geological criteria.
[b] Mean regional field direction derived from young lava units in the Sivas Basin (Piper et al., 2006).

expressed in the short term (10^3–10^5 years) as PSV and occasional excursions, and in the long term (10^5–10^6 years) by reversals of polarity can provide a timescale for ancient earthquakes provided that these same events are expressed in a rock succession with recoverable primary magnetism. Since travertine is the natural deposit most directly related to earthquake activity and is shown here to possess a palaeomagnetic record comparable to PSV, it is potentially a key tool in palaeoseismology if magnitudes of earthquakes producing the layering can be identified.

Historic seismic activity in the Sivas Basin has been included in the assessments of a number of authors (e.g. Ambraseys and Jackson, 1998; Gençoğlu et al., 1990) and damaging earthquakes were observed at Sivas in 1695 and in the Kayseri district to the SW at ~1745 (Ambraseys and Finkel, 1995). A high frequency of smaller earthquakes is evident from the density of normal faults cutting Quaternary alluvial deposits bordering the nearby Kızılırmak River (Gürsoy et al., 1992). Earthquake epicentres highlight a NE–SW trend of major faults delineating block boundaries. These record predominantly strike slip motions resulting from the south westward extrusion of terranes in central Anatolia by tectonic escape (Fig. 21; Piper et al., 2006). Mesci (2004) has compiled a record of observatory recorded earthquakes and identifies more than 50 earthquakes in this region of magnitudes (M) ≤4 between 1995 and 2002. Clearly earthquakes of this size range occur much too frequently to have significantly influenced travertine formation. Twelve earthquakes with magnitudes between 4 and 4.8 occurred between 1929 and 2005 and 5 earthquakes with magnitudes between 5.5 and 6.3 occurred between 1909 and 1939. Since only a few of these events would have occurred sufficiently close to influence the geothermal field it seems likely that events in the magnitude range ~4.5–5.5 are those capable of setting the reservoir and instigating a revitalised water flow.

There are two further signatures for the incidence of less frequent but much larger earthquakes within the record of travertine deposition in this geothermal field. These are firstly the incidental emplacement of massive travertine and fracturing of older travertine without destroying the fissure as a venue of travertine emplacement; these effects are observed by emplacement of massive travertine in the central part of Fissure 2 and by the truncation of earlier travertine noted in Fissure 1. The second is the termination of the fissure as a site of deposition with transfer of geothermal activity to a new fracture.

Earthquakes of comparable magnitudes that occur repeatedly on fault zones within similar time period are defined as "characteristic earthquakes". The resulting fault displacements, slip rates and magnitudes may then be assumed to be approximately constant and under such conditions the average recurrence period is related to the slip rate and earthquake magnitude. The relationship between earthquake magnitude and fault offset in the Basin and Range Province of western North America has been used by Slemmons and De Polo (1986) to derive the recurrence time of earthquakes as shown in Fig. 22. The model relates the average recurrence time to the ratio of the displacement per event and the slip rate on the assumption that if an $M = 7$ earthquake is characterised by a 1 m displacement, then an $M = 8$ event is equivalent to a proportional 5 m displacement, etc. Applying the results of this study to this empirical relationship enables an estimate of earthquake magnitude and frequency responsible for the second and most catastrophic type of earthquake event in the Sıcak Çermik field to be made. This approach is valid provided that repeated earthquakes on the fault segment occur with similar magnitudes and displacements (Schwartz and Coppersmith, 1984, Keller and Pinter, 1996). The palaeomagnetic analysis indicates a minimum life of ~2000 years for fissure duration here (Fissure 1) with age spans at the base of the mounds being likely to be in the range 5000–10,000

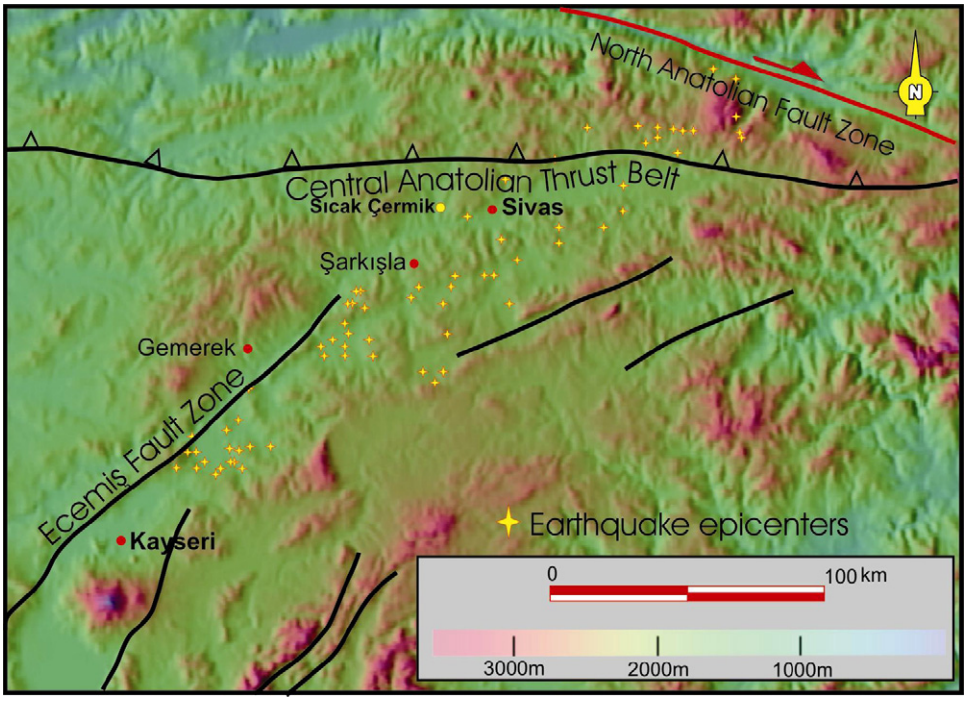

Fig. 21. The region of the Sivas Basin bordering the Sıcak Çermik geothermal field showing epicentres of $M \geq 4$ 20th century earthquakes.

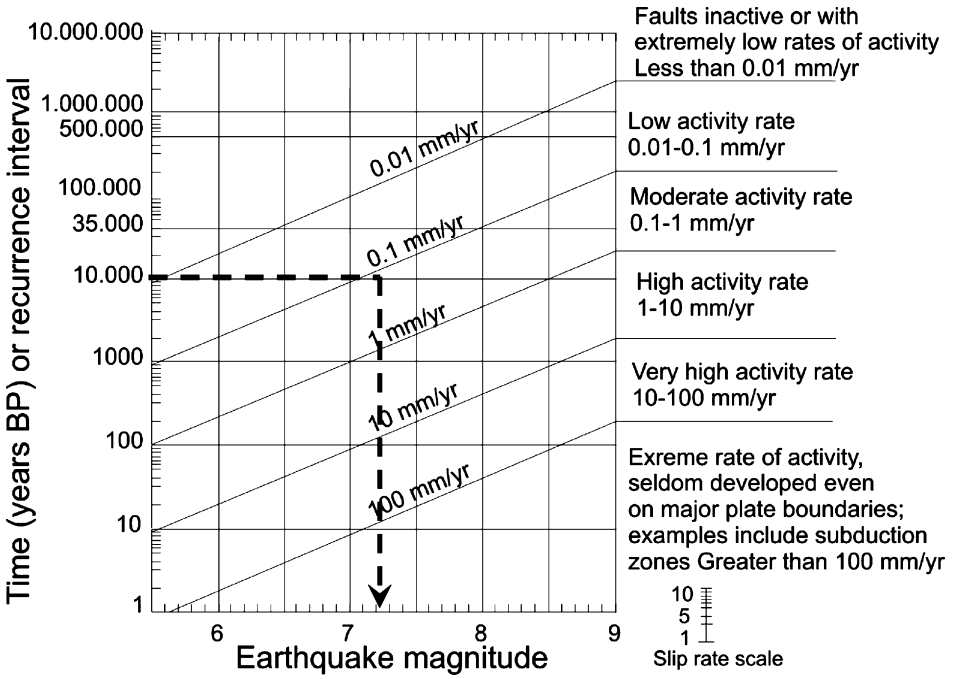

Fig. 22. Relationship between earthquake magnitude and fault offset used to estimate the recurrence time of earthquakes in western North America after Keller and Pinter (1996). The estimated average life span of a travertine fissure and the typical rate of fissure opening are estimated from the palaeomagnetic study (see text) and suggest that occasional earthquakes of magnitude 7–8 are responsible for terminating a travertine fissure and generating a new hydrothermal system.

(Fissure 3) years, a figure independently suggested by the overall number of fissures in the Sıcak Çermik field noted above. The extension rate determined from the palaeomagnetic correlation with PSV ranges from 0.2 to 0.6 mm/year (contributed from growth on both sides of fissures 1, 2 and 3). Entering these two constraints in Fig. 22 indicates that a magnitude $M \sim 7.5$ event about every 10,000 years could record the extreme of earthquake activity in this region (presumably on the block bounding faults, see Fig. 20) and be responsible for shifting the geothermal activity to a new fracture.

10. Conclusions

This investigation has primarily aimed to evaluate the use of travertine as a recorder of PSV, environmental change and earthquake frequency. A coherent record of the ancient magnetic field has been resolved from the material studied here, with the exception of most of the bedded travertine at localities 4 and 5 at Sıcak Çermik which yielded few coherent components with thermal demagnetisation, and the massive travertine in Fissure 2 which failed to record the direction of the presumed ambient field. Both types of travertine otherwise show temporal variations in direction reminiscent of PSV, although shallowing of inclination is recognised in the bedded travertine. The examples of PSV resolved here are too old to be of value for correlation with archaeomagnetic and geomagnetic investigations in the eastern Mediterranean region, but they do show that investigations of younger travertine deposits elsewhere should be of value in this context provided that the age of deposition is constrained. The recognition of cycles in the PSV signature provides a means of estimating the rate of travertine growth which cannot be reliably achieved from the U–Th dating due to the magnitude of errors associated with the latter application.

Although temporal variations in ferromagnetic content are observed within travertine, its corresponding value as a geomagnetic proxy for palaeoenvironment remains obscure. Magnetic susceptibilities and intensities of magnetisation across the fissures studied here vary by one and two orders of magnitude, respectively, and there are some systematic variations on either side of the axes (Figs. 6 and 7) but no apparent correlation with colour. This may be because much of the brown staining is actually due to paramagnetic organic complexes incorporated within the travertine (e.g. Latham and Ford, 1993). Thus the rock magnetic results of this study yield no definitive conclusions on the environmental significance of travertine although such a signature is likely to be present because changes in the input of meteoric water will influence downward flushing of the local terra rossa soil and nutrients contained within it. Iron carbonate is paramagnetic and apparently only a minor constituent of the travertine, whilst the ferromagnets are particulate and presumably sourced in the soil. The latter input might be expected to be more abundant during pluvial periods which should therefore correlate with peaks of susceptibility (Figs. 6 and 7). However, the signature will be modulated by groundwater supply, which is likely to be starved during dry periods. Also, an application of magnetic susceptibility employing the relationship evident in Fig. 10 will be the signature of changes in chemistry and partial pressures within the hydrothermal reservoir and cannot effectively be applied until the climatic significance of aragonite versus calcite deposition is resolved.

However, the pursuit of a palaeoclimate record in layered and fissure travertine is probably a worthwhile objective both because of the large volume of material available for study and because of the potential for correlating with the stratigraphic record of PSV (Section 7). The bedded travertine has a distinct magnetic record of atmospheric origin and can show major susceptibility signatures (Fig. 19); it is therefore a potential recorder of volcanic events and prevailing wind input.

Travertine is the natural deposit most closely linked to the regional earthquake signature and can therefore yield a palaeomagnetic record of value to palaeoseismological investigation. Since both fissure and bedded travertine yield records of the palaeomagnetic field direction compatible with the signature of PSV, a temporal link to earthquake frequency can be based on the assumption that cycles of PSV were similar to those resolved from archaeological and historical records during the past few thousands of years. By counting the number of travertine layers within a cycle of PSV we have a means of estimating the frequency of earthquakes capable of resetting the reservoir. The typical magnitudes of the earthquake events responsible for influencing the travertine deposition can then be estimated from the historical records.

Two larger but more incidental signatures of earthquake activity are illustrated by the occasional emplacement of massive travertine and by the initiation of new travertine fissures. Travertine can thus provide an indication of bimodality in earthquake magnitude/frequency and indicate sourcing from two or more levels and stress regimes within the crust.

Acknowledgements

We are grateful to the British Council, NATO (Grant No: CLG-EST-977055) and TUBITAK (Grant

YDABAG 101Y023) for supporting palaeomagnetic and neotectonic investigations in Turkey and for promoting the link between the Department of Geology at the Cumhuriyet University and the Geomagnetism Laboratory at Liverpool. We are also very grateful to Abigail Bull, Clare Ward and Mohamed Alyaroubi for their contributions to the laboratory studies during undergraduate project investigations.

References

Ambraseys, N.N., Finkel, C.F., 1995. Seismicity of Turkey and Adjacent Areas: An Historical Catalogue of Earthquakes 1500–1799. Eren Publishing House, Istanbul, p. 240.

Ambraseys, N.N., Jackson, J.A., 1998. Faulting associated with historical and recent earthquakes in the Eastern Mediterranean region. Geophys. J. Int. 133, 390–406.

Ayaz, E., Gökçe, A., 1998. Geology and genesis of the Sıcak Çermik, Sarıkaya and Uyuz Çermik travertine deposits northwest of Sivas, Turkey. Bull. Faculty Eng. Cumhuriyet Univ., A 15, 1–12.

Butler, R.F., 1992. Palaeomagnetism: Magnetic Domains to Geologic Terranes. Blackwell, Oxford, p. 319.

Chang, S.R., Kirschvink, J.L., 1989. Magnetofossils, the magnetisation of sediments and the evolution of magnetite biomineralisation. Annu. Rev. Earth Planet. Sci. 17, 169–195.

Dearing, J.A., Dann, R.J.L., Hay, K., Lees, J.A., Loveland, P.J., Maher, B.A., O'Grady, K., 1996. Frequency-dependent susceptibility measurements of environmental materials. Geophys. J. Int. 124, 228–240.

Duchi, V., Giordano, M.V., Martini, M., 1978. Riesame del problema della precipitatzione di calcite od aragonite da soluzioni naturali. Rend. Soc. Ital. Mineral. Petrol. 34, 605–618.

Gençoğlu, S., İnan, E., Güler, H.H., 1990. Turkiye'nin Deprem Tehlikesi. Publ. Chamber of Geophysical Engineering of Turkey, p. 701.

Gürsoy, H., Temiz, H., Poisson, A., 1992. Recent faulting in the Sivas area (Sivas Basin, Central Anatolia—Turkey). Bull. Faculty Eng. Cumhuriyet Univ., A 9, 11–17.

Gürsoy, H., Piper, J.D.A., Tatar, O., Temiz, H., 1997. A palaeomagnetic study of the Sivas basin, Central Turkey: crustal deformation during lateral extrusion of the Anatolian block. Tectonophysics 271, 89–105.

Hancock, P.L., Chalmers, R.M.L., Altunel, E., Cakir, Z., 1999. Travitonics: using travertines in active fault studies. J. Struct. Geol. 21, 903–916.

Keller, E.A., Pinter, N., 1996. Active Tectonics. Prentice Hall, New Jersey, p. 338.

Latham, A.G., Ford, D.C., 1993. The palaeomagnetism and rock magnetism of cave and karst deposits. In: Aissaoui, D.M., Hurley, N.F., Lidz, B.H. (Eds.), Applications of Palaeomagnetism to Sedimentary Geology, vol. 49, pp. 149–155 (SEPM Special Publication).

Marton, P., 1996. Archaeomagnetic directions: the Hungarian calibration curve. In: Morris, A., Tarling, D.H. (Eds.), Palaeomagnetism and Tectonics of the Mediterranean Region, vol. 105. Geol. Soc. Spec. Publ., pp. 385–399.

Mesci, B.L., 2004. The Development of Travertine occurences in Sıcak Çermik, Delikkaya and Sarıkaya (Sivas) and their Relationships to Active Tectonics. PhD thesis. Cumhuriyet University, Sivas, Turkey, p. 245 (Unpublished, in Turkish with English abstract).

Mesci, B.L., Gursoy, H., Tatar, O., 2007. The development of travertine deposits in Sıcak Çermik, Delikkaya and Sarıkaya (Sivas), Central Turkey, and their relationship to active tectonics, Turkish J. Earth Sci., in press.

Piper, J.D.A., Tatar, O., Gursoy, H., 1997. Deformational behaviour of continental lithosphere deduced from block rotations across the North Anatolian fault zone in Turkey. Earth Planet. Sci. Lett. 150, 191–203.

Piper, J.D.A., Tatar, O., Gürsoy, H., Koçbulut, F., Mesci, B.L., 2006. Palaeomagnetic Analysis of Neotectonic Deformation in the Anatolian Accretionary Collage, Turkey, vol. 409. Geological Society of America, pp. 417–440 (special publication).

Robertson, D.J., France, D.E., 1994. Discrimination of remanence-carrying minerals in mixtures, using isothermal remanent magnetisation acquisition curves. Phys. Earth Planet. Interiors 82, 223–234.

Şengör, A.M.C., Yılmaz, Y., 1981. Tethyan evolution of Turkey: a plate tectonic approach. Tectonophysics 75, 181–241.

Schwartz, D.P., Coppersmith, K.J., 1984. Fault behaviour and characteristic earthquakes: examples from the Wasatch and San Andreas Fault Zones. J. Geophys. Res. 89, 5681–5698.

Slemmons, D.B., De Polo, C.M., 1986. Evaluation of Active Faulting and Associated Hazards, Active Tectonics. National Academy Press, Washington, DC.

Tarling, D.H., 1988. Secular variations of the geomagnetic field—the archaeomagnetic record. In: Stevenson, F.R., Wolfendale, A.W. (Eds.), Secular, Solar and Geomagnetic Variation in the Last 10,000 Years. Kluwer Academic Publishers, pp. 349–365.

Tatar, O., Piper, J.D.A., Gürsoy, H., Temiz, H., 1996. Regional significance of neotectonic anticlockwise rotation in central Turkey. Int. Geol. Rev. 38, 692–700.

Thompson, R., Oldfield, F., 1986. Environmental Magnetism. Allen and Unwin, London, p. 227.

Turi, B., 1986. Stable isotope geochemistry of travertines. In: Fritz, P., Fontes, J.C. (Eds.), Handbook of Environmental Isotope Geochemistry. Elsevier, Amsterdam, pp. 207–238.

Van Hinszberger, D.J.J., Langereis, C.G., Meulenkamp, J.E., 2005. Revision of the timing, magnitude and distribution of Neogene rotations in the western Aegean region. Tectonophysics 396, 1–34.